**EPJ C manuscript No.**
(will be inserted by the editor)



**LU 2001/027, LPNHE 2001-14**

# New method for calculating helicity amplitudes of jet–like QED processes for high–energy colliders I. Bremsstrahlung processes

C. Carimalo[1a], A. Schiller[2,b], and V.G. Serbo[3,c]

[1] LPNHE, IN2P3-CNRS, Université Paris VI, F-75252 Paris, France
[2] Institut für Theoretische Physik and NTZ, Universität Leipzig, D-04109 Leipzig, Germany
[3] Novosibirsk State University, Novosibirsk, 630090 Russia

Received: December 19, 2001

**Abstract.** Inelastic QED processes, the cross sections of which do not drop with increasing energy, play an important role at high–energy colliders. Such reactions have the form of two–jet processes with the exchange of a virtual photon in the $t$-channel. We consider them in the region of small scattering angles $m/E \lesssim \theta \ll 1$, which yields the dominant contribution to their total cross sections. A new effective method is presented and applied to QED processes with emission of real photons to calculate the helicity amplitudes of these processes. Its basic idea is similar to the well–known equivalent–lepton method. Compact analytical expressions for those amplitudes up to $e^8$ are derived omitting only terms of the order of $m^2/E^2$, $\theta^2$, $\theta m/E$ and higher order. The helicity amplitudes are presented in a compact form in which large compensating terms are already cancelled. Some common properties for all jet–like processes are found and we discuss their origin.

## 1 Introduction

### 1.1 Subject of the paper

Accelerators with high-energy colliding $e^+e^-$, $\gamma e$, $\gamma\gamma$ and $\mu^+\mu^-$ beams are now widely used or designed to study fundamental interactions [1]. Some processes of quantum electrodynamics (QED) might play an important role at these colliders, especially those inelastic processes the cross section of which do not drop with increasing energy. For this reason and since, in principle, the planned colliders will be able to work with polarized particles, these QED processes are required to be described in full detail, including the calculation of their amplitudes with definite helicities of all initial and final particles — leptons ($l = e$ or $\mu$) and photons $\gamma$. These reactions have the form of a two–jet process with the exchange of a virtual photon $\gamma^*$ in the $t$-channel (Fig. 1).

We define by a jet kinematics in QED a high–energy reaction in which the outgoing particles (leptons and photons) are produced within a small cone $\theta_i \ll 1$ relative to the propagation axis of their respective parental incoming particle. We work in the collider reference frame in which the initial particles with 4-momenta $p_1$ and $p_2$ perform a head–on collision with respective energies $E_1$ and $E_2$ of the same order. The subject of our consideration is the jet–like process of Fig. 1 at high energies ($m_i$ is a lepton mass)

$$s = 2p_1p_2 = 4E_1E_2 \gg m_i^2 \tag{1}$$

for arbitrary helicities of leptons $\lambda_i = \pm 1/2$ and photons $\Lambda_i = \pm 1$. The emission and scattering angles $\theta_i$ are allowed to be much smaller than unity though they may be of the order of the typical emission angles $m_i/E_i$ or larger. Stated differently, the transverse momenta of final particles $\mathbf{p}_{i\perp}$ are allowed to be of the order of the lepton mass or larger:

$$\frac{m_i}{E_i} \lesssim \theta_i \ll 1\,, \quad m_i \lesssim |\mathbf{p}_{i\perp}| \ll E_i\,. \tag{2}$$

The processes under discussion have large total cross sections. Therefore, they present an essential background and they determine particle losses in the beams and the beam life time. Since all these processes can be calculated

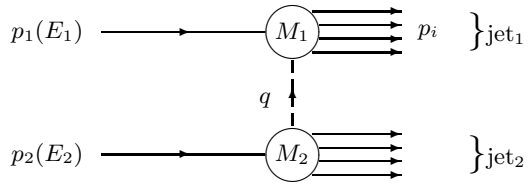


**Fig. 1.** Generic block diagram of the two–jet process $ee \to \text{jet}_1\ \text{jet}_2$.

[a] carimalo@in2p3.fr
[b] Arwed.Schiller@itp.uni-leipzig.de
[c] serbo@math.nsc.ru

with high accuracy independently of any model of strong interaction, they can usefully serve for monitoring luminosity and polarization of colliding beams. Besides, there is a specific feature exhibited by some of jet–like processes — the so-called MD or beam–size effect (see review [2] for detail).

All these properties of the jet–like QED processes justify the growing interest to them from both the experimental and theoretical communities in high–energy physics. Particular problems related to these processes were discussed in a number of original papers [3]–[24] and in reviews such as [25,26,2]. But only recently (see Ref. [24]) the highly accurate analytical calculation of the helicity amplitudes of all jet–like processes up to $e^4$ (shown in Figs. 2–10) has been completed.

In the above–mentioned original papers different approaches and notations have been used. Here we develop a new simple and effective method to calculate jet–like processes and apply it to QED processes with emission of real photons. In particular, we consider in detail the case of emission of up to three photons along the direction of the initial particle (Fig. 11).

It is quite important to realize that at high energies (1) the region of scattering angles (2) gives the dominant contribution to the cross sections of all QED jet–like processes such as those shown in Figs. 2–11. Just in this region the amplitudes of these processes can be found in a "final form" including the polarizations of all particles. By this we mean that we obtain compact and simple analytical expressions for all helicity amplitudes with high accuracy, omitting only terms of the order of

$$\frac{m_i^2}{E_i^2}\ ,\quad \theta_i^2\ ,\quad \theta_i\cdot\frac{m_i}{E_i} \tag{3}$$

or higher order. Namely, the amplitude $M_{fi}$ of any process given in Figs. 1–11 can be presented in a simple factorized form

$$M_{fi}=\frac{s}{q^2}J_1J_2 \tag{4}$$

where the impact factors $J_1$ and $J_2$ do not depend on $s$. The impact factor $J_1$ corresponds to the first jet (or the upper block) and the impact factor $J_2$ corresponds to the second jet (or the lower block) of Fig. 1.

We give analytical expressions for these impact factors. They are not only compact but are also very convenient for numerical calculations. The reason is that we present the impact factors in such a form that large compensating terms are already cancelled. It is well known that this problem of large compensating terms is very difficult to manage in all computer packages like CompHEP [27] which generate automatically matrix elements and compute cross sections.

It should be noted that the discussed approximation differs considerably from the known approach of the CALCUL group and others [28] where such processes are calculated for not too small scattering angles $\theta_i \gg m_i/E_i$. In that approach terms of the order of $m_i/|\mathbf{p}_{i\perp}|$ are neglected, which, however, may give the dominant contribution to the total cross sections.

To get the high–energy helicity amplitudes in the jet–like kinematics as compact analytical expressions and to make the calculations very efficient we systematically exploit three basic ideas: (i) a convenient decomposition of all 4–momenta into large and small components (using the so–called Sudakov or light–cone variables); (ii) gauge invariance of the amplitudes is used in order to combine large terms into finite expressions; (iii) the calculations are considerably simplified in replacing the numerators of lepton propagators by vertices involving real leptons and antileptons. All these ideas are not new. In particular, the last one is the basis of the equivalent–lepton method [4,14, 22] and has been used to calculate some QCD amplitudes with massless quarks [29]. However, as we will demonstrate in the present paper, the combination of these ideas leads to a very efficient way in calculating the amplitudes of interest in the jet kinematics here considered.

### 1.2 Jet–like QED processes up to fourth order with nondecreasing cross sections

We consider electromagnetic interactions of electrons, positrons and photons on tree-level in high–energy $ee$, $e\gamma$ and $\gamma\gamma$ collisions. To third and fourth orders in the electromagnetic coupling $e$ the corresponding jet–like QED processes in the form of block diagrams are shown in Figs. 2–10. Solid lines represent leptons, dashed one photons. Only those diagrams are drawn that give the dominant contributions at high energies.

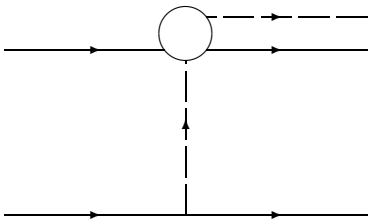

**Fig. 2.** Single bremsstrahlung in $ee$ collisions: $ee \to ee\gamma$.

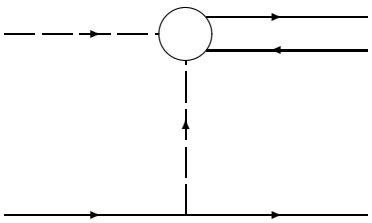

**Fig. 3.** Single lepton pair production in $\gamma e$ collisions: $\gamma e \to l^+l^-e$.

The third order processes are: single bremsstrahlung in $e^{\pm}e$ collision (Fig. 2) and single lepton pair $l^+l^-$ production in $\gamma e$ collision (Fig. 3). To the fourth order processes belong lepton pair production and bremsstrahlung in various combinations, including simple combinations of the above–mentioned third order processes (Figs. 4–6) and new types of reactions (Figs. 7–10).

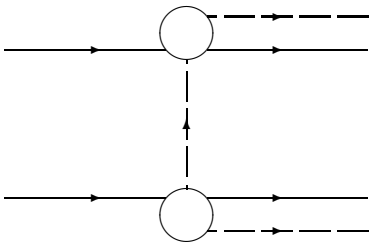

**Fig. 4.** Double bremsstrahlung with single photons along each initial lepton direction: $ee \to ee\gamma\gamma$.

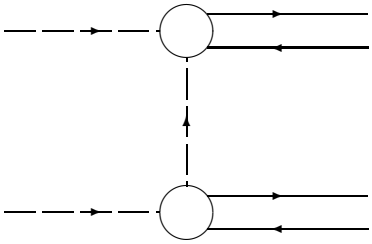

**Fig. 5.** Double lepton pair production in $\gamma\gamma$ collisions: $\gamma\gamma \to e^+e^-l^+l^-$.

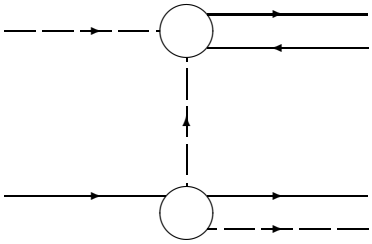

**Fig. 6.** Process $\gamma e \to l^+l^-e\gamma$ with a final photon along the initial lepton direction.

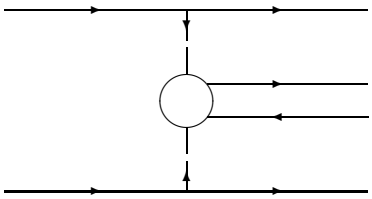

**Fig. 7.** Two–photon pair production in $ee$ collisions: $ee \to ee\, l^-l^+$.

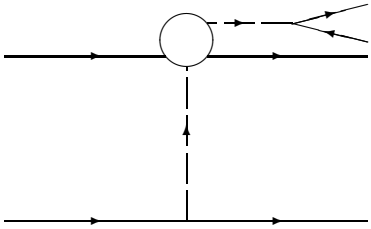

**Fig. 8.** Bremsstrahlung pair production in $ee$ collisions: $ee \to ee\, l^+l^-$.

The discussed processes are important for the following reasons:

1) Some of these reactions are used (or are proposed to be used) as monitoring processes to determine the collider luminosity and to measure the polarization of the colliding particles. For example, the double bremsstrahlung process (Fig. 4) has been used as the standard calibration process at several colliders in Novosibirsk, Frascati and Orsay [30,31]. In Ref. [32] it has been suggested to use the single bremsstrahlung process (Fig. 2) for measuring the luminosity and the polarization of the initial $e^\pm$ at the LEP collider (see also paper [33]). As it was demonstrated experimentally (see Ref. [34]), that process has a good chance to be used for luminosity purposes. The same process has been proposed [35] to measure the luminosity at the DA$\Phi$NE collider (see also Ref. [36]). The processes $\gamma\gamma \to \mu^+\mu^-e^+e^-$ and $\gamma\gamma \to \mu^+\mu^-\mu^+\mu^-$ of Fig. 5 may be useful to monitor colliding $\gamma\gamma$ beams [37, 20,38]. Finally, the possibility of designing $\mu^+\mu^-$ colliders is widely discussed at present. Therefore, the processes $\mu^+\mu^- \to l^+l^-l^+l^-$ $(l = e, \mu)$ may be useful for luminosity measurements at those colliders [39]. Recently, processes of Figs. 7 and 8 have been taken into account as radiative corrections to the unpolarized Bhabha scattering used as calibration process at LEP [40].

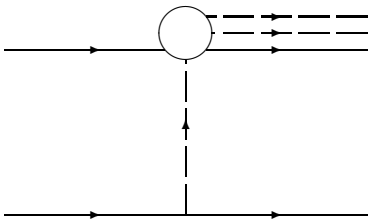

**Fig. 9.** Double bremsstrahlung $ee \to ee\gamma\gamma$ with two photons along the direction of one initial lepton.

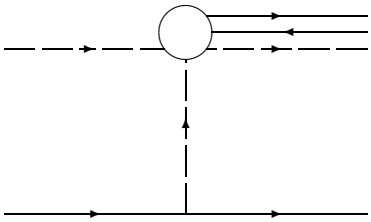

**Fig. 10.** Process $\gamma e \to \gamma l^+l^-e$ with the both final photon and lepton pair along the direction of the initial photon.

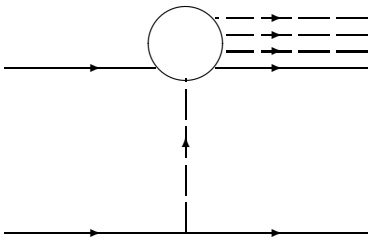

**Fig. 11.** Triple bremsstrahlung $ee \to ee\gamma\gamma\gamma$ with three photons along the direction of one initial lepton.

2) Due to their large cross sections those reactions contribute as significant background to a number of experiments in the electroweak sector and to hadronic cross sections. For example, the background process $e^+e^- \to e^+e^-\mu^+\mu^-$ is of special importance for experiments study-

ing two–photon and bremsstrahlung production of $\pi^+\pi^-$ systems due to the known experimental difficulties in discriminating pions and muons [41].

3) The bremsstrahlung process of Fig. 2 is of special importance for storage rings since it is the leading beam loss mechanism: after emitting a photon with energy above approximately 1 %, the electron leaves the beam. Therefore, the luminosity and the beam life time of the $e^+e^-$ storage rings depends strongly on the properties of this reaction [42].

4) The methods to calculate the helicity amplitudes of these processes and to obtain some distributions for the latter can be easily translated to several semihard QCD processes such as $\gamma\gamma \to q\bar{q}Q\bar{Q}$ [20] ($q$ and $Q$ are different quarks) and $\gamma\gamma \to MM'$, $\gamma\gamma \to Mq\bar{q}$ [43] ($M, M'$ denote neutral mesons such as $\rho^0$, $\omega$, $\phi$, $\Psi$, $\pi^0$, $a_2$...).

The outline of the paper is as follows. In Sect. 2 we describe the method for the calculation of the helicity amplitudes. In the next section we derive all vertices necessary for the bremsstrahlung processes and discuss their properties. Sections 4–6 are devoted to the calculation of the impact factors for single, double and multiple bremsstrahlung. Some general properties of the impact factors are discussed in Sect. 7. The final chapter summarizes our results. In the Appendix we collect some formulae for the Dirac bispinors and matrices in the so–called spinor or chiral representation that appears to be useful for calculation in the region of small angles.

## 2 Method for calculation of helicity amplitudes

### 2.1 Sudakov or light-cone variables

Let us introduce some notations using the block diagram of Fig. 1 for example. We use a collider reference frame with the $z$–axis along the momentum $\mathbf{p}_1$, the azimuthal angles are denoted by $\varphi_i$ (they are referred to one fixed $x$-axis). It is convenient to introduce the light-like 4–vectors $P_1$ and $P_2$:

$$\begin{aligned} &P_1 = p_1 - \frac{m_1^2}{sa}\,p_2,\ \ P_2 = p_2 - \frac{m_2^2}{sa}\,p_1,\ \ P_1^2 = P_2^2 = 0\,,\\ &s = 2p_1p_2,\\ &\tilde{s} = (P_1+P_2)^2 = 2P_1P_2 = s\left(1 - \frac{4\epsilon}{a} + \frac{\epsilon}{a^2}\right), \qquad (5)\\ &a = \frac{1}{2}\left(1+\sqrt{1-4\epsilon}\right) \approx 1-\epsilon\,,\ \ \epsilon = \frac{m_1^2m_2^2}{s^2} \end{aligned}$$

and to decompose any 4–vector $A$ into components in the plane spanned by the 4–vectors $P_1$ and $P_2$ and components in the plane orthogonal to them

$$\begin{aligned} &A = x_AP_1 + y_AP_2 + A_\perp\,,\ \ A^2 = \tilde{s}x_Ay_A + A_\perp^2\,,\\ &x_A = \frac{2AP_2}{\tilde{s}}\,,\ \ y_A = \frac{2AP_1}{\tilde{s}}\,. \qquad (6) \end{aligned}$$

The parameters $x_A$ and $y_A$ are the so-called *Sudakov variables* (they often are referred also as *light-cone variables*). In the used reference frame

$$\begin{aligned} &P_1 = E_1a_1\,(1,\,0,\,0,\,1)\,,\ \ P_2 = E_2a_2\,(1,\,0,\,0,\,-1)\,,\\ &a_i = 1 - \frac{m_i^2}{E_i^2a} \approx 1 - \frac{m_i^2}{E_i^2} \end{aligned}$$

and the 4–vector $A_\perp$ has $x$ and $y$ components only, e.g.

$$A_\perp = (0,\,A_x,\,A_y,\,0) = (0,\,\mathbf{A}_\perp,\,0)\,,\quad A_\perp^2 = -\mathbf{A}_\perp^2\,.$$

Omitting terms of the order of $\epsilon$ only, we have

$$\tilde{s} = s\,,\ \ A^2 = sx_Ay_A - \mathbf{A}_\perp^2\,,\ \ x_A = \frac{2AP_2}{s}\,,\ \ y_A = \frac{2AP_1}{s}\,.$$

For the colliding particles the Sudakov variables are

$$x_1 = 1\,,\ \ y_1 = \frac{m_1^2}{s}\,,\ \ x_2 = \frac{m_2^2}{s}\,,\ \ y_2 = 1\,. \qquad (7)$$

We also note the useful relation for all external momenta

$$p_i^2 = m_i^2 = sx_iy_i - \mathbf{p}_{i\perp}^2 \qquad (8)$$

which means that for each external momentum only three parameters are independent (say, $x_i$ and $\mathbf{p}_{i\perp}$ for the first jet).

The 4–vectors $p_i$ of particles from the first jet have large components along $P_1$ and small ones along $P_2$. Therefore, in the limit $s \to \infty$ [with accuracy (3)] the parameters

$$x_i = \frac{2p_iP_2}{s} = \frac{E_i}{E_1}\,,\ \ i \in \text{ jet}_1 \qquad (9)$$

are finite, whereas

$$y_i = \frac{2p_iP_1}{s} = \frac{m_i^2 + \mathbf{p}_{i\perp}^2}{sx_i}\,,\ \ i \in \text{ jet}_1 \qquad (10)$$

are small. The Sudakov variable $x_i$ is the fraction of energy of the first incoming particle carried by the $i$-th final particle. Analogously, for a 4–vector $p_l$ of particles from the second jet the parameters

$$y_l = \frac{2p_lP_1}{s} = \frac{E_l}{E_2}\,,\ \ l \in \text{ jet}_2 \qquad (11)$$

are finite, whereas

$$x_l = \frac{2p_lP_2}{s} = \frac{m_l^2 + \mathbf{p}_{l\perp}^2}{sy_l}\,,\ \ l \in \text{ jet}_2 \qquad (12)$$

are small. The parameter $y_l$ is the fraction of energy of the second initial particle carried by the $l$-th final particle. Since

$$x_q = x_2 - \sum_{l\in\text{jet}_2} x_l\,,\quad y_q = \sum_{i\in\text{jet}_1} y_i - y_1\,,$$

the Sudakov parameters for the virtual photon are small and, therefore,

$$\sum_{i\in\text{jet}_1} x_i = x_1 = 1\,,\ \ \sum_{l\in\text{jet}_2} y_l = y_2 = 1\,. \qquad (13)$$

Now we discuss the Sudakov decomposition of the photon polarization vector, using a final photon from the first jet for example. We would like to remind that we have chosen a coordinate system with a fixed $x$-axis transverse to the beam direction. Let $e \equiv e^{(\Lambda)}(k)$ be the polarization 4-vector of that photon with 4–momentum $k$ and helicity $\Lambda = \pm 1$. Using gauge invariance, this vector can be replaced by $e + \zeta k$. The arbitrary parameter $\zeta$ is chosen in such a way that the new polarization vector (for which we use the same notation $e$) has no a component along $P_1$, i.e.

$$e = y_e P_2 + e_\perp \,. \tag{14}$$

The parameter $y_e$ is determined from the condition $ek = 0$:

$$s y_e = \frac{-2k_\perp e_\perp}{x_k} \,, \quad x_k = \frac{2kP_2}{s} \,. \tag{15}$$

Since $P_2 P_2 = P_2 e_\perp = 0$, the transverse component $e_\perp$ satisfies the usual normalization condition

$$e_\perp^{(\Lambda)\,*} e_\perp^{(\Lambda')} = e^{(\Lambda)\,*}(k)\, e^{(\Lambda')}(k) = -\delta_{\Lambda\Lambda'}$$

and can be chosen as

$$e_\perp \equiv e_\perp^{(\Lambda)} = -\frac{\Lambda}{\sqrt{2}} \,(0,\, 1,\, \mathrm{i}\Lambda,\, 0) = -e_\perp^{(-\Lambda)\,*} \,. \tag{16}$$

Therefore, $e_\perp$ does not depend on the 4–momentum of the photon $k$ contrary to the polarization vector $e$ itself which depends on $k$ via the parameter $y_e$. This, indeed, is very convenient in the further calculations since we can choose the same form of the transverse 4–vector $e_\perp$ for all final photons in the first jet. For the photon with helicity $\tilde{\Lambda}$ and polarization vector $\tilde{e} = \tilde{x}_e P_1 + \tilde{e}_\perp$ in the second jet we use the relation

$$\tilde{e}_\perp^{(\tilde{\Lambda})} = e_\perp^{(-\tilde{\Lambda})} \,. \tag{17}$$

In the following we systematically neglect terms of the relative order of (3).

### 2.2 Helicity amplitudes in factorized form

The amplitude $M_{fi}$ corresponding to the diagram of Fig. 1 can be written in the form

$$M_{fi} = M_1^\mu \; \frac{g_{\mu\nu}}{q^2} \; M_2^\nu, \tag{18}$$

where $M_1^\mu$ and $M_2^\nu$ are the amplitudes of the upper and lower block of Fig. 1, respectively, and $g_{\mu\nu}$ is the metric tensor. The transition amplitude $M_1$ describes the scattering of an incoming particle of momentum $p_1$ with a virtual photon and subsequent transition to the first jet (similar for $M_2$).

We will show now that the amplitude of the process can be presented with accuracy (3) in factorized form:

$$M_{fi} \,=\, \frac{s}{q^2}\, J_1\, J_2 \,,$$

$$J_1 = \frac{\sqrt{2}}{s}\, M_1^\mu \, P_{2\mu} \,, \qquad J_2 = \frac{\sqrt{2}}{s}\, M_2^\nu \, P_{1\nu} \,. \tag{19}$$

In the limit $s \to \infty$ the quantity $J_1$ ($J_2$), called impact factor, can be calculated, assuming that the energy fractions $x_i$ ($y_l$) and transverse momenta of the final particles $\mathbf{p}_{i\perp}$ ($\mathbf{p}_{l\perp}$) remain finite. Therefore, the impact factor $J_1$ depends on $x_i$, $\mathbf{p}_{i\perp}$ with $i \in$ jet$_1$ and on the helicities of the first particle and of the particles in the first jet. Note that the impact factor $J_1$ ($J_2$) results from the contraction of the corresponding amplitude with the light–like 4–vector $P_2$ ($P_1$).

To show the factorization, we present the metric tensor $g_{\mu\nu}$ in the form

$$\begin{aligned} g^{\mu\nu} &= \frac{(P_1+P_2)^\mu (P_1+P_2)^\nu}{(P_1+P_2)^2} + \\ &+ \frac{(P_1-P_2)^\mu (P_1-P_2)^\nu}{(P_1-P_2)^2} + g_\perp^{\mu\nu} = \\ &= \frac{2(P_2^\mu P_1^\nu + P_1^\mu P_2^\nu)}{\tilde{s}} + g_\perp^{\mu\nu} \,. \end{aligned} \tag{20}$$

The first equality can be easily checked in the cms where $P_1 = (\sqrt{\tilde{s}}/2)(1,0,0,1)$ and $P_2 = (\sqrt{\tilde{s}}/2)(1,0,0,-1)$. Note that Eqs. (20) are exact. Using this expression for the metric tensor in Eq. (18), we obtain the amplitude as a sum of three terms

$$\begin{aligned} M_{fi} = &\frac{2}{\tilde{s}q^2} \; (M_1^\mu P_{2\mu}) \; (M_2^\nu P_{1\nu}) + \\ &+ \frac{2}{\tilde{s}q^2} \; (M_1^\mu P_{1\mu}) \; (M_2^\nu P_{2\nu}) + M_1^\mu \frac{g_{\perp\,\mu\nu}}{q^2} M_2^\nu \,. \end{aligned} \tag{21}$$

Let us estimate the contribution of each of these terms to $M_{fi}$. The amplitude $M_1^\mu$ of the upper block depends on the momentum of the first particle $p_1$, on the momenta $p_i$ of the particles in the first jet and on the momentum $q$ of the virtual photon. Since $p_1$ and $p_i$ have large components along $P_1$ and small components along $P_2$ and $q$ has small components both along $P_1$ and along $P_2$, one obtains the estimates

$$M_1^\mu P_{1\mu} \propto s^0 \,, \quad M_1^\mu P_{2\mu} \propto s \tag{22}$$

and analogously

$$M_2^\nu P_{1\nu} \propto s \,, \quad M_2^\nu P_{2\nu} \propto s^0 \,. \tag{23}$$

By virtue of these estimates, only the first term in Eq. (21) can give a contribution proportional to $s$. As a result, we can use the representation (19) for the amplitude of the process.

It is useful to point out another form of Eq. (19). Due to gauge invariance of the amplitude with respect to the virtual photon we have

$$q_\mu M_1^\mu = (x_q P_1 + y_q P_2 + q_\perp)_\mu \, M_1^\mu = 0 \,. \tag{24}$$

Taking into account that $x_q$ is small, one finds $x_q P_{1\mu} \, M_1^\mu \propto 1/s$, whereas $y_q P_{2\mu} \, M_1^\mu \propto s^0$ and $q_{\perp\mu} \, M_1^\mu \propto s^0$ what leads to

$$M_1^\mu \, P_{2\mu} = -M_1^\mu \, \frac{q_{\perp\,\mu}}{y_q} \,. \tag{25}$$

Analogously, we find for the second amplitude $M_2^\mu P_{1\mu} = -M_2^\mu q_{\perp\mu}/x_q$. Therefore, we can represent the impact factors in the form

$$J_1 = -\frac{\sqrt{2}}{sy_q}\, M_1^\mu\, q_{\perp\,\mu}\,, \quad J_2 = -\frac{\sqrt{2}}{sx_q}\, M_2^\nu\, q_{\perp\,\nu}\,. \tag{26}$$

In other words, up to a factor $\left[-\sqrt{-2q_\perp^2}/(sy_q)\right]$, the impact factor $J_1$ coincides with an amplitude describing the scattering of the first incoming particle with the virtual photon of "mass" squared $q^2$ and polarization 4–vector $q_{\perp\,\mu}/\sqrt{-q_\perp^2}$.

The representations (26) of the impact factors are very important. They show that at small transverse momentum of the exchanged photon both impact factors should behave as

$$J_{1,2} \propto |\mathbf{q}_\perp| \;\text{ at }\; \mathbf{q}_\perp \to 0\,. \tag{27}$$

In our further analysis we will combine various contributions of the impact factor into expressions which clearly exhibit such a behavior. The detailed properties of the impact factors are described in Sections 4–7.

### 2.3 Vertices instead of spinor lines

Let us consider a virtual electron in the amplitude $M_1$ with 4–momentum $p = (E, \mathbf{p})$, energy $E > 0$ and virtuality $p^2 - m^2$. Due to jet kinematics, its virtuality is small, $|p^2 - m^2| \ll E^2$. We introduce an artificial energy

$$E_p = \sqrt{m^2 + \mathbf{p}^2}$$

and the bispinors $u_{\mathbf{p}}^{(\lambda)}$ and $v_{\mathbf{p}}^{(\lambda)}$ corresponding to a real electron and a real positron with 3–momentum $\mathbf{p}$ and energy $E_p$ (the exact expressions for these bispinors are given in the Appendix). In the high-energy limit this artificial energy is close to the true one:

$$\frac{E - E_p}{E + E_p} = \frac{p^2 - m^2}{(E + E_p)^2} \approx \frac{p^2 - m^2}{4E^2}\,. \tag{28}$$

Since

$$\begin{aligned} u_{\mathbf{p}}^{(\lambda)}\bar{u}_{\mathbf{p}}^{(\lambda)} &= E_p\gamma^0 - \mathbf{p}\boldsymbol{\gamma} + m\,, \\ v_{-\mathbf{p}}^{(\lambda)}\bar{v}_{-\mathbf{p}}^{(\lambda)} &= E_p\gamma^0 + \mathbf{p}\boldsymbol{\gamma} - m\,, \end{aligned} \tag{29}$$

we have the exact identity for the numerator of a virtual electron [14]:

$$\hat{p} + m = \frac{E + E_p}{2E_p}\, u_{\mathbf{p}}^{(\lambda)}\bar{u}_{\mathbf{p}}^{(\lambda)} + \frac{E - E_p}{2E_p}\, v_{-\mathbf{p}}^{(\lambda)}\bar{v}_{-\mathbf{p}}^{(\lambda)} \tag{30}$$

where summation over the helicities $\lambda = \pm 1/2$ is understood. Taking into account the approximation (28), we will use this expression in the simpler form[1]

$$\hat{p} + m \approx u_{\mathbf{p}}^{(\lambda)}\bar{u}_{\mathbf{p}}^{(\lambda)} + \frac{p^2 - m^2}{4E^2}\, v_{-\mathbf{p}}^{(\lambda)}\bar{v}_{-\mathbf{p}}^{(\lambda)}\,. \tag{31}$$

Moreover, since

$$v_{-\mathbf{p}}^{(\lambda)}\bar{v}_{-\mathbf{p}}^{(\lambda)} = E_p\gamma^0 + \mathbf{p}\boldsymbol{\gamma} - m = x_v\hat{P}_1 + y_v\hat{P}_2 + \hat{p}_\perp - m$$

with the Sudakov variables (in the given accuracy)

$$x_v = \frac{m^2 - p_\perp^2}{4EE_1}, \;\; y_v = \frac{E}{E_2}\,,$$

we can present that numerator $\hat{p} + m$ in another form

$$\hat{p} + m \approx u_{\mathbf{p}}^{(\lambda)}\bar{u}_{\mathbf{p}}^{(\lambda)} + \frac{p^2 - m^2}{4EE_2}\,\hat{P}_2\,. \tag{32}$$

Omitting terms of the order of (3) or higher, the expressions (31), (32) are exact.

Using Eq. (31) for all virtual electrons (of small virtuality) appearing in the impact factors , we are able to substitute the numerators of all spinor propagators by transition currents (or generalized vertices) involving real electrons and real positrons. As we will show in the next section, those generalized vertices are finite in the limit $s \to \infty$. On the contrary, a numerator like $\hat{p} + m$ is in that limit a sum of a finite term $\hat{p}_\perp + m$ and an unpleasant combination $E\gamma^0 - p_z\gamma_z$ of large terms that requires special care. Therefore, those replacements significantly simplify all calculations of the impact factors $J_i$.

Let us notice some important technical points when calculating spinor products appearing in the impact factors:

1) If an electron line with numerator $\hat{p} + m$ connects vertices with the emission of one real and one virtual photon, we have the following spinor structure around $\hat{p} + m$

$$\hat{e}^*\,(\hat{p} + m)\,\hat{P}_2 \quad \text{or} \quad \hat{P}_2\,(\hat{p} + m)\,\hat{e}^*\,.$$

In this particular case (using Eq. (32) and taking into account $\hat{P}_2\,\hat{P}_2 = 0$) we obtain the simple substitution rule

$$\hat{p} + m \to u_{\mathbf{p}}^{(\lambda)}\bar{u}_{\mathbf{p}}^{(\lambda)}\,. \tag{33}$$

From that discussion it is obvious that within accuracy (3) the following possible generalized vertices

$$\bar{v}_{-\mathbf{p}'}^{(\lambda')}\,\hat{P}_2\,v_{-\mathbf{p}}^{(\lambda)} \tag{34}$$

will not appear in the calculation of impact factors.

[1] Analogously, for the numerator of the propagator for a virtual positron with 4–momentum $p = (E, \mathbf{p})$ and energy $E > 0$ we find the form

$$\hat{p} - m \approx v_{\mathbf{p}}^{(\lambda)}\bar{v}_{\mathbf{p}}^{(\lambda)} + \frac{p^2 - m^2}{4E^2}\, u_{-\mathbf{p}}^{(\lambda)}\bar{u}_{-\mathbf{p}}^{(\lambda)}\,.$$

2) A vertex with an emission of a real photon, $\hat{e}^*$, has the "environment"

$$(\hat{p}' + m)\,\hat{e}^*\,(\hat{p} + m)\,.$$

If we use Eq. (31) in the form $\hat{p} + m = \hat{a} + \hat{b}$ and $\hat{p}' + m = \hat{a}' + \hat{b}'$ with $\hat{a} = u^{(\lambda)}_{\mathbf{p}} \bar{u}^{(\lambda)}_{\mathbf{p}}$, $\hat{b} = (p^2 - m^2)\, v^{(\lambda)}_{-\mathbf{p}} \bar{v}^{(\lambda)}_{-\mathbf{p}} / (4E^2)$ and similar expressions for $\hat{a}'$, $\hat{b}'$, we obtain four terms:

$$(\hat{p}' + m)\,\hat{e}^*\,(\hat{p} + m) = \hat{a}'\,\hat{e}^*\,\hat{a} + \hat{a}'\,\hat{e}^*\,\hat{b} + \hat{b}'\,\hat{e}^*\,\hat{a} + \hat{b}'\,\hat{e}^*\,\hat{b}\,.$$

The last term in this expression is zero, what can be shown as follows: using for $\hat{b}$ the form $\hat{b} = (p^2 - m^2)\,\hat{P}_2/(4EE_2)$ [see Eq. (32)], and a similar one for $\hat{b}'$, and taking into account Eq. (14), one finds

$$\hat{b}'\,\hat{e}^*\,\hat{b} \propto \hat{P}_2\,\hat{e}^*\,\hat{P}_2 = \hat{P}_2\,\left(y_e \hat{P}_2 + \hat{e}_\perp\right)^*\,\hat{P}_2 = 0\,. \qquad (35)$$

From that observation we conclude that in the calculations of the impact factors generalized vertices of the type

$$\bar{v}^{(\lambda')}_{-\mathbf{p}'}\,\hat{e}^*\,v^{(\lambda)}_{-\mathbf{p}} \qquad (36)$$

are also absent.

3) It is easy to check that

$$\bar{u}^{(\lambda')}_{\mathbf{p}'}\,\hat{e}^*\,v^{(\lambda)}_{-\mathbf{p}} = \bar{v}^{(\lambda')}_{-\mathbf{p}'}\,\hat{e}^*\,u^{(\lambda)}_{\mathbf{p}}\,.$$

4) Due to the absence of vertices (34) and (36) generalized vertices of "exchange" type can appear only in pairs (changing the electron state to positron states with negative 3–momentum and back to an electron state) in the subsequent emission of two real photons.

## 3 Vertices for bremsstrahlung processes

### 3.1 The $e(p) \to e(p') + \gamma(k)$ and $e(p) + \gamma^*(q) \to e(p')$ transitions

To calculate the impact factors involving the emission of real photons we need only two types of vertices: those for the transition $e(p) \to e(p') + \gamma(k)$ where $\gamma(k)$ is a real photon with helicity $\Lambda$ and the vertex for the transition $e(p) + \gamma^*(q) \to e(p')$ where $\gamma^*(q)$ is a virtual photon with energy fraction $x_q = 0$ (within our accuracy).

The following vertices belong to the first type[2]:

$$V(p,\,k) \equiv V^{\Lambda}_{\lambda\lambda'}(p,\,k) = \bar{u}^{(\lambda')}_{\mathbf{p}'}\,\hat{e}^{(\Lambda)\,*}\,u^{(\lambda)}_{\mathbf{p}}\,, \qquad (37)$$

$$\tilde{V}(p,\,k) \equiv \tilde{V}^{\Lambda}_{\lambda\lambda'}(p,\,k) = \bar{u}^{(\lambda')}_{\mathbf{p}'}\,\hat{e}^{(\Lambda)\,*}\,v^{(\lambda)}_{-\mathbf{p}} = \bar{v}^{(\lambda')}_{-\mathbf{p}'}\,\hat{e}^{(\Lambda)\,*}\,u^{(\lambda)}_{\mathbf{p}}\,. \qquad (38)$$

[2] We define the vertices as follows: in writing the amplitude or impact factor from left to right we follow the electron line from its beginning to its end. In our case this is more natural than going in the opposite direction along the electron line as usually done.

Certainly, the calculation of these vertices does not depend on the concrete representation of bispinors and $\gamma$-matrices, but it is very convenient to use the spinor representation described in the Appendix. The result of calculation with accuracy (3) is the following

$$V(p,\,k) = \Big[\delta_{\lambda\lambda'}\,2\,\left(e^{(\Lambda)\,*}p\right)\,(1 - x\,\delta_{\Lambda,-2\lambda}) + \\ +\,\delta_{\lambda,-\lambda'}\,\delta_{\Lambda,2\lambda}\,\sqrt{2}\,mx\Big]\,\Phi\,, \qquad (39)$$

$$\tilde{V}(p,\,k) = -2\sqrt{2}\,\Lambda\,E'\,\delta_{\lambda,-\lambda'}\,\delta_{\Lambda,2\lambda}\,\Phi \qquad (40)$$

where

$$x = \frac{\omega}{E}\,, \quad \Phi = \sqrt{\frac{E}{E'}}\,\mathrm{e}^{\mathrm{i}(\lambda'\varphi' - \lambda\varphi)}\,. \qquad (41)$$

It is useful to remind here that for the polarization vectors $e$ [see Eq. (14)] we have

$$ep = e_\perp\,\left(p_\perp - \frac{k_\perp}{x}\right)\,. \qquad (42)$$

The vertex of the second type is very simple:

$$V(p) \equiv V_{\lambda\lambda'}(p) = \frac{\sqrt{2}}{s}\,\bar{u}^{(\lambda')}_{\mathbf{p}'}\,\hat{P}_2\,u^{(\lambda)}_{\mathbf{p}} = \sqrt{2}\,\frac{E}{E_1}\,\delta_{\lambda\lambda'}\,\Phi\,. \qquad (43)$$

Let us make some general remarks related to Eqs. (39)–(43):

1) We have previously mentioned [after Eq. (19)] that the impact factors remain finite in the high–energy limit $s \to \infty$. Now we observe from (39), (42) and (43) that the vertices $V(p,k)$ and $V(p)$ are finite in that limit too. Due to properties 3) and 4) discussed in Sect. 2.3 the "exchange" vertices $\tilde{V}$ appear only in combinations $[(p^2 - m^2)/(4E^2)]\tilde{V}(p - k_i, k_i)\tilde{V}(p, k_{i+1})$ which also remain finite. Indeed, the factor $p^2 - m^2$ (denominator of the considered lepton propagator between neighbouring real photons) gives the finite virtuality in the high energy limit, the $1/E^2$ factor combines with the energies $E$ and $E' = E - \omega_{i+1}$ according to Eq. (38) to an energy independent factor. All calculations are exact up to neglected pieces of the order of (3).

2) For the bremsstrahlung of $n$ real photons along an electron line, the production of factors $\Phi$, corresponding to the emission of $n$ real photons and one virtual photon,

$$\Phi_1\Phi_2 ... \Phi_n\Phi_q = \sqrt{\frac{E_1}{E_3}}\,\mathrm{e}^{\mathrm{i}(\lambda_3\varphi_3 - \lambda_1\varphi_1)} \qquad (44)$$

is proportional to a phase factor which can be included in the definition of the corresponding amplitude. Therefore, in the calculation of this amplitude we can omit all factors $\Phi$ appearing in Eqs. (39), (40), (43).

3) Up to now we have considered the bremsstrahlung by electrons. It is quite natural that the presented formulae are also valid for the bremsstrahlung by positrons. Let us consider, for example, the vertex $\bar{v}^{(\lambda)}_{\mathbf{p}}\,\hat{e}^{(\Lambda)\,*}\,v^{(\lambda')}_{\mathbf{p}'}$ which corresponds to the $e^+(p) \to e^+(p') + \gamma(k)$ transition. If we

take into account the relations for bispinors

$$v^{(\lambda')}_{\mathbf{p}'} = C\,\left(\bar{u}^{(\lambda')}_{\mathbf{p}'}\right)^T\,, \tag{45}$$
$$\bar{v}^{(\lambda)}_{\mathbf{p}} = \left(C\,u^{(\lambda)}_{\mathbf{p}}\right)^T = \left(u^{(\lambda)}_{\mathbf{p}}\right)^T\,C^T = -\left(u^{(\lambda)}_{\mathbf{p}}\right)^T\,C^{-1}$$

and $\gamma$ matrices

$$C^{-1}\hat{e}^{(\Lambda)\,*}C = -\left(\hat{e}^{(\Lambda)\,*}\right)^T \tag{46}$$

(here the matrix $C=\gamma^2\gamma^0$ is related to the charge conjugation operator, see Appendix), we immediately obtain

$$\bar{v}^{(\lambda)}_{\mathbf{p}}\,\hat{e}^{(\Lambda)\,*}\,v^{(\lambda')}_{\mathbf{p}'} = \bar{u}^{(\lambda')}_{\mathbf{p}'}\,\hat{e}^{(\Lambda)\,*}\,u^{(\lambda)}_{\mathbf{p}} \equiv V(p,\,k)\,. \tag{47}$$

### 3.2 Helicity conserved and helicity non–conserved vertices

In the further calculations we need only formulae (37)–(44). But for reference reasons it is convenient to rewrite them for some particular cases, omitting the factors $\Phi$.

In the case of the helicity conserved (HC) transitions, $\lambda'=\lambda$, the vertices are of the form:

$$V(p,k) = 2e^*p \qquad \text{for} \quad \Lambda = 2\lambda = 2\lambda'\,, \tag{48}$$
$$V(p,k) = 2e^*p\,(1-x) \quad \text{for} \quad \Lambda = -2\lambda = -2\lambda'\,, \tag{49}$$
$$V(p) = \sqrt{2}\,E/E_1\,, \tag{50}$$
$$\tilde{V}(p,k) = 0 \tag{51}$$

and additionally [taking into account Eq. (42)]

$$2e^{(+)*}p = \sqrt{2}\,z^*\,,\;\; 2e^{(-)*}p = -\sqrt{2}\,z\,,$$
$$z = p_x + \mathrm{i}p_y - \frac{k_x+\mathrm{i}k_y}{x}\,. \tag{52}$$

In the case of the helicity non–conserved (HNC) transitions, $\lambda'=-\lambda$, we have:[3]

$$V^+_{+-}(p,k) = V^-_{-+}(p,k) = \sqrt{2}\,mx\,, \tag{53}$$
$$\tilde{V}^+_{+-}(p,k) = -\tilde{V}^-_{-+}(p,k) = -2\sqrt{2}\,E'\,, \tag{54}$$
$$V^-_{+-}(p,k) = V^+_{-+}(p,k) = \tilde{V}^-_{+-}(p,k) = \tilde{V}^+_{-+}(p,k) = V_{+-}(p) = V_{-+}(p) = 0\,. \tag{55}$$

### 3.3 Properties of vertices

From the derived expressions for the vertices the following properties can be found:

1) Vertices with a maximal change of helicity,

$$\max|\Delta\lambda| = \max|\Lambda+\lambda'-\lambda| = 2\,, \tag{56}$$

are absent what can be seen from Eqs. (55). This property as well as property 4) below are a result of the conservation of the total angular momentum $J_z$ in the strict forward direction. Indeed, the vertices for HNC transitions do not depend on the transverse momenta of the particles in the jet. Therefore, they do not change for transitions setting all transverse momenta to zero. In other words, those vertices can be calculated for the case of strict forward emission for which the total angular momentum is conserved: $J_z=\lambda=\Lambda+\lambda'$.

2) If the produced photon becomes very hard ($\omega\to E$) the initial electron "transmits" its helicity to the photon:

$$V(p,k)\propto\delta_{\Lambda,2\lambda}\,,\quad \tilde{V}(p,k)\to 0 \quad \text{for} \quad x\to 1\,. \tag{57}$$

3) If the final electron becomes hard ($E'\to E$, soft photon limit, $x\ll 1$), the initial electron "transmits" its helicity to the final electron: in that limit the vertex

$$V(p,k) = -\frac{2}{x}\,(e^*_\perp\,k_\perp)\;\delta_{\lambda\lambda'} \tag{58}$$

dominates, which corresponds to the approximation of a classical current.

4) For HNC vertices a strong correlation between the helicities of the initial electron and the photon exists:

$$\Lambda = 2\lambda \quad \text{if} \quad \lambda' = -\lambda\,. \tag{59}$$

For HC vertices there is no strong correlation between helicities of electrons and the photon (excluding the limiting case of $\omega\to E$).

5) From Eqs. (48), (49), (52) it can be seen that

$$V^+_{\lambda\lambda}\propto z^*\,,\;\; V^-_{\lambda\lambda}\propto z \tag{60}$$

where $z$ is defined in Eq. (52).

## 4 Impact factor for the single bremsstrahlung $e(p_1)+\gamma^*(q)\to e(p_3)+\gamma(k)$

The impact factor for the single bremsstrahlung corresponds to the virtual Compton scattering (Fig. 12) where

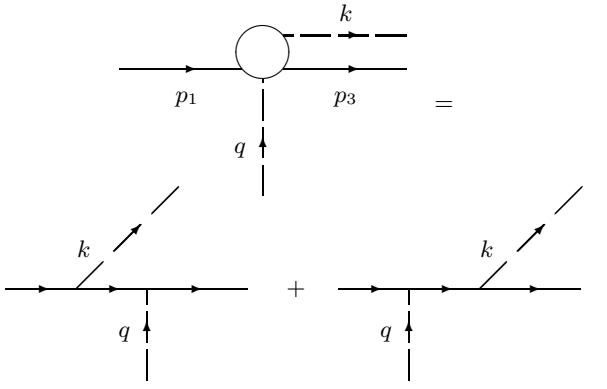


**Fig. 12.** Amplitude for the virtual Compton scattering.

[3] Here and in the following we use the sign notation both for the photon polarization $\Lambda=\pm1=\pm$ and the lepton helicity $\lambda=\pm1/2=\pm$.

$J_1$ is given as follows:

$$J_1(e_{\lambda_1}+\gamma^*\to e_{\lambda_3}+\gamma_\Lambda)=4\pi\alpha\left(\frac{N_1}{2p_1k}-\frac{N_3}{2p_3k}\right) \quad (61)$$

with

$$N_1=\bar u_3\frac{\sqrt{2}\hat P_2}{s}\,(\hat p_1-\hat k+m)\hat e^*u_1\,,$$
$$N_3=\bar u_3\hat e^*(\hat p_3+\hat k+m)\frac{\sqrt{2}\hat P_2}{s}\,u_1\,, \quad (62)$$

$e\equiv e^{(\Lambda)}(k)$ is the polarization 4-vector of the final photon. Here for $\hat p_1-\hat k+m$ and $\hat p_3+\hat k+m$ we can use the simple substitution (33) that allows us to eliminate the numerators of the two spinor propagators and to introduce the vertices $V(p)$ and $V(p,k)$.

The vertices $V(p)$ are diagonal in the helicity basis and simply lead to factors $\sqrt{2}\,(1-x)$ with $x=\omega/E_1$ for $N_1$ and $\sqrt{2}$ for $N_3$. As a result, we have

$$J_1=\sqrt{2}\,4\pi\alpha\,\left[\frac{1-x}{2p_1k}V(p_1,k)-\frac{1}{2p_3k}\,V(p_3+k,k)\right]\,\Phi\,, \quad (63)$$

with the vertices (remind that $e^{(\Lambda)\,*}\,k=0$)

$$V(p_1,\,k)=\delta_{\lambda_1\lambda_3}\,2\,\left(e^{(\Lambda)\,*}p_1\right)\,(1-x\,\delta_{\Lambda,-2\lambda_1})+$$
$$+\,\delta_{\lambda_1,-\lambda_3}\,\delta_{\Lambda,2\lambda_1}\,\sqrt{2}\,mx\,, \quad (64)$$
$$V(p_3+k,\,k)=\delta_{\lambda_1\lambda_3}\,2\,\left(e^{(\Lambda)\,*}p_3\right)\,(1-x\,\delta_{\Lambda,-2\lambda_1})+$$
$$+\,\delta_{\lambda_1,-\lambda_3}\,\delta_{\Lambda,2\lambda_1}\,\sqrt{2}\,mx$$

and the $\Phi$ factor in the form of Eq. (44)

$$\Phi=\frac{1}{\sqrt{1-x}}\,\mathrm{e}^{\mathrm{i}(\lambda_3\varphi_3-\lambda_1\varphi_1)}\,. \quad (65)$$

From Eq. (63) it is clear that the properties of $J_1$ are determined by the properties of the vertices described in Sect. 3.3. In the soft photon limit, $x\ll 1$, we have the usual approximation by classical currents:

$$J_1=\sqrt{2}\,4\pi\alpha\,\left(\frac{e^*p_1}{p_1k}-\frac{e^*p_3}{p_3k}\right)\,\Phi\,\delta_{\lambda_1\lambda_3}\,. \quad (66)$$

The impact factor $J_1$ can be transformed to a form which clearly exhibits the proportionality $J_1\propto q_\perp$ resulting from the gauge invariance of $J_1$ with respect to the virtual photon (see Eq. (27)). For this purpose we use Eqs. (64), (42) and rewrite

$$V(p_3+k,k)=V(p_1+q,k)=V(p_1,k)+ \quad (67)$$
$$+\,2\,\left(q_\perp\,e_\perp^{(\Lambda)\,*}\right)\,(1-x\,\delta_{\Lambda,-2\lambda_1})\,\delta_{\lambda_1\lambda_3}\,.$$

This gives the following result

$$J_1=\sqrt{2}\,4\pi\alpha\,\left[A_1\,V(p_1,k)+q_\perp B_1\right]\,\Phi\,, \quad (68)$$
$$A_1=\frac{1-x}{2p_1k}-\frac{1}{2p_3k}\,,\;B_1=-\frac{e_\perp^{(\Lambda)\,*}}{p_3k}\,(1-x\,\delta_{\Lambda,-2\lambda_1})\,\delta_{\lambda_1\lambda_3}\,.$$

The last term in $J_1$ is directly proportional to $q_\perp$ and it is not difficult to check that the same is true for the first term. Indeed, since

$$2p_1k=xa\,,\;\;a=\,m^2+\frac{\mathbf{k}_\perp^2}{x^2}\,,$$
$$2p_3k=\frac{x}{1-x}\,b\,,\;\;b=m^2+\left(\mathbf{q}_\perp-\frac{\mathbf{k}_\perp}{x}\right)^2\,,$$

we immediately obtain

$$A_1=\frac{1-x}{x}\,\left(\frac{1}{a}-\frac{1}{b}\right)\propto q_\perp\,. \quad (69)$$

As a result, Eq. (68) is a simple and compact expression for all 8 helicity states written in such a form that all individual large (compared to $q_\perp$) contributions are cancelled.

Let us discuss the form of $J_1$ for the single bremsstrahlung by a positron. We expect that the only difference is connected with the change of the charge sign $-e\to+e$ in each vertex with the emission of a real or virtual photon. In our case this gives the additional factor $(-1)^2=1$, therefore,

$$J_1\left(e^+_{\lambda_1}+\gamma^*\to e^+_{\lambda_3}+\gamma_\Lambda\right)=J_1\left(e^-_{\lambda_1}+\gamma^*\to e^-_{\lambda_3}+\gamma_\Lambda\right)\,. \quad (70)$$

To give the formal proof of this relation, we take into account that going over from electron to positron bremsstrahlung the numerators of the electron propagators $\hat p+m$ have to be replaced by $-\hat p+m$ for the positrons and the bispinors $u_1$ and $\bar u_3$ for the electrons by those for the positrons $\bar v_1$ and $v_3$. In addition , a factor $(-1)$ has to be added according to one of the Feynman rules[4]. It gives

$$J_1\left(e^+_{\lambda_1}+\gamma^*\to e^+_{\lambda_3}+\gamma_\Lambda\right)=(-1)\cdot 4\pi\alpha\,\left(\frac{\tilde N_1}{2p_1k}-\frac{\tilde N_3}{2p_3k}\right)$$

with

$$\tilde N_1=\bar v_1\,\hat e^*(-\hat p_1+\hat k+m)\frac{\sqrt{2}\hat P_2}{s}\,v_3\,,$$
$$\tilde N_3=\bar v_1\,\frac{\sqrt{2}\hat P_2}{s}\,(-\hat p_3-\hat k+m)\,\hat e^*v_3\,.$$

If we take into account (see Appendix and Eqs. (46), (46)) the relations for bispinors

$$(-1)\cdot\bar v_1=-\,(C\,u_1)^T=(u_1)^T\,C^{-1}\,,$$
$$v_3=C\,\left(\bar u_3\right)^T\,, \quad (71)$$

spinor propagators

$$C^{-1}(-\hat p+m)C=(\hat p+m)^T \quad (72)$$

[4] See, for example, rule (9) in text-book [45] §77: "An additional factor $-1$ is included in $\mathrm{i}M_{fi}$ for ... each pair of positron external lines if these are beginning and end of a single sequence of a lepton line."

and vertices for the real and virtual photons

$$C^{-1}\hat{e}^*C = -\,(\hat{e}^*)^T\,, \quad C^{-1}\hat{P}_2C = -\left(\hat{P}_2\right)^T \tag{73}$$

with the matrix $C=\gamma^2\gamma^0$, we immediately obtain Eq. (70).

The basic Eq. (63) can be rewritten in another form which may be useful in concrete calculations. If we take into account that

$$e^*p_1 = -\frac{e^*_\perp k_\perp}{x}\,,\;\; e^*p_3 = e^*(p_1+q) = e^*_\perp\left(q_\perp - \frac{k_\perp}{x}\right), \tag{74}$$

we arrive at the result of Ref. [21]:

$$\begin{aligned} &J_1(e_{\lambda_1}+\gamma^*\to e_{\lambda_3}+\gamma_\Lambda) = \\ &= 8\pi\alpha\frac{\sqrt{1-x}}{x}\,\mathrm{e}^{\mathrm{i}(\lambda_3\varphi_3-\lambda_1\varphi_1)}\times \\ &\left[(1-x\delta_{\Lambda,-2\lambda_1})\,\sqrt{2}\mathbf{T}\mathbf{e}^{(\Lambda)\,*}_\perp\,\delta_{\lambda_1\lambda_3} + m\,xS\delta_{\lambda_1,-\lambda_3}\delta_{\Lambda,2\lambda_1}\right] \end{aligned} \tag{75}$$

where the transverse 4–vector $T$ (in the used reference frame $T=(0,\mathbf{T},0)$, $T^2=-\mathbf{T}^2$) and the scalar $S$ are defined as

$$T = \frac{(k_\perp/x)}{a} + \frac{q_\perp-(k_\perp/x)}{b}\,,\quad S=\frac{1}{a}-\frac{1}{b} \tag{76}$$

with the useful relation

$$\mathbf{T}^2 + m^2S^2 = \frac{\mathbf{q}^2_\perp}{ab}\,. \tag{77}$$

Since

$$T\propto q_\perp\,,\quad S\propto q_\perp\,, \tag{78}$$

we again conclude that $J_1\propto q_\perp$.

## 5 Impact factor for the double bremsstrahlung $e(p_1)+\gamma^*(q)\to e(p_3)+\gamma(k_1)+\gamma(k_2)$

### 5.1 Notations

The impact factor for the double bremsstrahlung corresponds to six diagrams, three of them are shown in Fig. 13. We indicate explicitly the helicity states of the initial and final electrons $\lambda_{1,3}$ and of the final photons $\Lambda_{1,2}$[5]:

$$J_1 = \sqrt{2}\,(4\pi\alpha)^{3/2}\,X_3\,\mathcal{M}^{\Lambda_1\,\Lambda_2}_{\lambda_1\,\lambda_3}(x_1,x_2,k_{1\perp},k_{2\perp},p_{3\perp})\,\Phi \tag{79}$$

with

$$\Phi = \frac{1}{\sqrt{X_3}}\,\mathrm{e}^{\mathrm{i}(\lambda_3\varphi_3-\lambda_1\varphi_1)}\,. \tag{80}$$

Let us stress again that $J_1$ and $\mathcal{M}$ do not depend on $s$. They depend only on the energy fractions

$$x_{1,2}=\omega_{1,2}/E_1,\;\; X_3=E_3/E_1\,,\quad x_1+x_2+X_3=1$$

[5] Here the amplitude $\mathcal{M}$ differs from the same quantity used in Ref. [24] by a factor $S_{\lambda_{e3}}$.

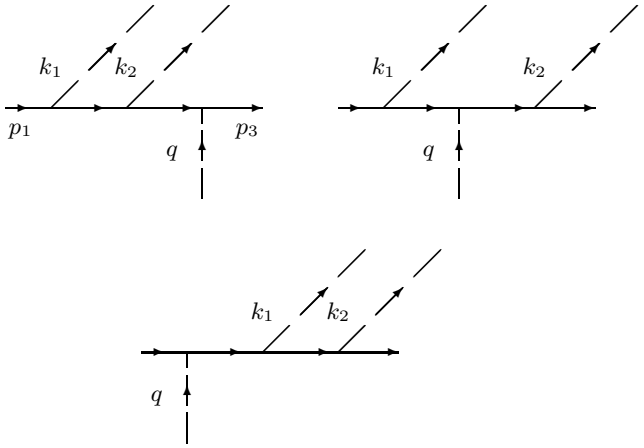


**Fig. 13.** Feynman diagrams for the impact factor related to the double bremsstrahlung, diagrams with $k_1\leftrightarrow k_2$ photon exchange have to be added.

and on the transverse momenta of the final particles in the first jet.

We also introduce the transverse vectors ($j=1,\,2$)

$$q_\perp = k_{1\perp}+k_{2\perp}+p_{3\perp}\,,\quad r_j=(X_3k_j-x_jp_3)_\perp\,, \tag{81}$$

and useful complex combinations of the transverse vector components [cf. Eq. (52)]

$$K_j = k_{jx}+\mathrm{i}\,k_{jy},\;\; Q=q_x+\mathrm{i}\,q_y,\;\; R_j=r_{jx}+\mathrm{i}\,r_{jy}\,. \tag{82}$$

The polarization 4-vectors $e_j\equiv e^{(\Lambda_j)}(k_j)$ for both final photons are chosen in the form (14)–(16).

The denominators of the propagators in Fig. 13 are expressed via the energy fractions and transverse momenta as follows:

$$\begin{aligned} a_j &\equiv -(p_1-k_j)^2+m^2 = \frac{1}{x_j}(m^2x_i^2+\mathbf{k}^2_{j\perp})\,, \\ b_j &\equiv (p_3+k_j)^2-m^2 = \frac{1}{x_jX_3}(m^2x_j^2+\mathbf{r}^2_{j\perp})\,, \\ a_{12}=a_{21} &\equiv -(p_1-k_1-k_2)^2+m^2 = \\ &= a_1+a_2-\frac{1}{x_1x_2}\,(x_1\mathbf{k}_{2\perp}-x_2\mathbf{k}_{1\perp})^2\,, \\ b_{12}=b_{21} &\equiv (p_3+k_1+k_2)^2-m^2 = \\ &= b_1+b_2+\frac{1}{x_1x_2}\,(x_1\mathbf{k}_{2\perp}-x_2\mathbf{k}_{1\perp})^2\,. \end{aligned} \tag{83}$$

### 5.2 General formula for the helicity amplitudes

Following the electron line from left to right in the Feynman diagrams in Fig. 13 and writing down the corresponding vertices, we immediately obtain the result for the impact factor $J_1$ or the amplitude $\mathcal{M}$ of Eq. (79). Moreover, if the electron line begins or ends at a vertex with the virtual photon (the first and last diagram of Fig. 13), we can

use the simple substitution (33) just as in Sect 4. In the other case we use the substitution rule (31). Therefore, for the first and the third diagrams we get contributions as products of two adjacent vertices with real photon emission from electrons with the simple vertex including the virtual photon. In the case of the second diagram we have only the product of two vertices with real photons emission from the electron and the $e\gamma^* \to e$ transition vertex located in between those vertices.

Taking into account that the $e\gamma^* \to e$ transition vertices $V(p)$ lead to energy fraction factors $\sqrt{2}\,X_3$, $\sqrt{2}\,(1-x_1)$ and $\sqrt{2}$ for the first, second and third diagram of Fig. 13, respectively, we find[6]

$$\mathcal{M} = (1+\mathcal{P}_{12})\; M, \tag{84}$$

$$\begin{aligned} X_3 M = {} & \frac{X_3}{a_1 a_{12}}\, V(p_1,k_1)\, V(p_1-k_1,k_2) - \\ & - \frac{1-x_1}{a_1 b_2}\, V(p_1,k_1)\, V(p_1-k_1+q,k_2) + \\ & + \frac{1}{b_{12} b_2}\, V(p_1+q,k_1)\, V(p_1-k_1+q,k_2) - \\ & - \frac{X_3}{a_{12}}\, \frac{\tilde V(p_1,k_1)\, \tilde V(p_1-k_1,k_2)}{4(E_1-\omega_1)^2} + \\ & + \frac{1}{b_{12}}\, \frac{\tilde V(p_1+q,k_1)\, \tilde V(p_1-k_1+q,k_2)}{4(E_3+\omega_2)^2}\,. \end{aligned} \tag{85}$$

The permutation operator $\mathcal{P}_{12}$ for the photons is defined as

$$\mathcal{P}_{12} f(k_1,e_1;k_2,e_2) = f(k_2,e_2;k_1,e_1)\,, \qquad \mathcal{P}_{12}^2 = 1.$$

Now we transform $J_1$ to a form which clearly exhibits the proportionality $J_1 \propto q_\perp$. Using the following properties of vertices

$$\begin{aligned} V(p_1+q,k_1) &= V(p_1,k_1) + \\ &\quad + 2\left(e_\perp^{(\Lambda_1)\,*}\, q_\perp\right)\,(1-x_1\,\delta_{\Lambda_1,-2\lambda_1})\;\delta_{\lambda_1\lambda}\,, \\ V(p_1-k_1,k_2) &= V(p_1-k_1+q,k_2) - 2\left(e_\perp^{(\Lambda_2)\,*}\, q_\perp\right) \\ &\quad \times \left(1-\frac{x_2}{1-x_1}\,\delta_{\Lambda_2,-2\lambda}\right)\,\delta_{\lambda\lambda_3}\,, \\ \tilde V(p_1+q,k_1) &= \tilde V(p_1,k_1)\,, \\ \tilde V(p_1-k_1+q,k_2) &= \tilde V(p_1-k_1,k_2)\,. \end{aligned} \tag{86}$$

we obtain the result[7]:

$$\begin{aligned} X_3 M_{\lambda_1\,\lambda_3}^{\Lambda_1\Lambda_2} = {} & A_2\, V_{\lambda_1\lambda}^{\Lambda_1}(p_1,k_1)\, V_{\lambda\lambda_3}^{\Lambda_2}(p_1-k_1+q,k_2) + \\ & + q_\perp B_{2\,\lambda_1\,\lambda_3}^{\Lambda_1\Lambda_2} + \\ & + \tilde A_2 \frac{\tilde V_{\lambda_1\lambda}^{\Lambda_1}(p_1,k_1)\, \tilde V_{\lambda\lambda_3}^{\Lambda_2}(p_1-k_1,k_2)}{4E_1^2(1-x_1)^2} \end{aligned} \tag{87}$$

with the scalars

$$A_2 = \frac{X_3}{a_1 a_{12}} - \frac{1-x_1}{a_1 b_2} + \frac{1}{b_{12} b_2}\,, \quad \tilde A_2 = -\frac{X_3}{a_{12}} + \frac{1}{b_{12}} \tag{88}$$

and the transverse 4–vector $B_2$

$$\begin{aligned} B_{2\,\lambda_1\,\lambda_3}^{\Lambda_1\Lambda_2} = {} & -X_3\, \frac{2e_\perp^{(\Lambda_2)\,*}}{a_1 a_{12}}\, V_{\lambda_1\lambda_3}^{\Lambda_1}(p_1,k_1) \\ & \times \left(1-\frac{x_2}{1-x_1}\,\delta_{\Lambda_2,-2\lambda_3}\right) + \\ & + \frac{2e_\perp^{(\Lambda_1)\,*}}{b_{12} b_2}\, V_{\lambda_1\lambda_3}^{\Lambda_2}(p_1-k_1+q,k_2)\;(1-x_1\,\delta_{\Lambda_1,-2\lambda_1})\,. \end{aligned} \tag{89}$$

It is not difficult to check that the quantities $A_2$ and $\tilde A_2$ vanish in the limit of small $q_\perp$:

$$A_2 \propto q_\perp\,, \quad \tilde A_2 \propto q_\perp\,, \tag{90}$$

whereas $B_2$ is finite in this limit.

Let us stress that Eq. (84) together with relation (87) represents a very simple and compact expression for all 16 helicity states, where all individual large (compared to $q_\perp$) contributions have been rearranged into finite expressions.

### 5.3 Explicit expressions for the helicity amplitudes

Due to the parity conservation relation

$$\mathcal{M}_{-\lambda_1\,-\lambda_3}^{-\Lambda_1\,-\Lambda_2} = -(-1)^{\lambda_1+\lambda_3}\left(\mathcal{M}_{\lambda_1\,\lambda_3}^{\Lambda_1\Lambda_2}\right)^*\,, \tag{91}$$

there are only 8 independent helicity states of $\mathcal{M}$ among the whole set of 16. We fix the choice of the independent amplitudes by fixing the helicity of the initial electron to $\lambda_1 = +1/2 = +$. To find the amplitudes with given initial and final helicities, we start from Eq. (87) and substitute there the expressions for vertices taken from Eqs. (48), (49), (52)–(55).

Using the complex combinations (82) we immediately obtain the amplitudes $M$:

$$\begin{aligned} M_{++}^{++} &= 2\left\{A_2\frac{K_1^* R_2^*}{x_1 x_2 X_3} + \frac{K_1^* Q^*}{x_1 a_1 a_{12}} - \frac{Q^* R_2^*}{x_2 X_3 b_{12} b_2}\right\}\,, \\ M_{++}^{--} &= X_3\left(M_{++}^{++}\right)^*\,, \end{aligned} \tag{92}$$

$$\begin{aligned} M_{++}^{-+} = {} & -2(1-x_1) \\ & \times \left(A_2\frac{K_1 R_2^*}{x_1 x_2 X_3} + \frac{K_1 Q^*}{x_1 a_1 a_{12}} - \frac{Q R_2^*}{x_2 X_3 b_{12} b_2}\right)\,, \end{aligned} \tag{93}$$

$$\begin{aligned} M_{++}^{+-} = {} & \frac{X_3}{(1-x_1)^2}\left(M_{++}^{-+}\right)^* + \\ & + \frac{2}{1-x_1}\left(m^2 A_2 \frac{x_1 x_2}{X_3} - \tilde A_2\right)\,, \end{aligned} \tag{94}$$

[6] Let us remind that $M$, $V$ and $\tilde V$ are matrices with respect to lepton helicities, in particular,

$$M = M_{\lambda_1\,\lambda_3}^{\Lambda_1\,\Lambda_2}\,,\;\; V(p,k_1) = V_{\lambda_1\,\lambda}^{\Lambda_1}(p,k_1)\,,\;\; V(p,k_2) = V_{\lambda\,\lambda_3}^{\Lambda_2}(p,k_2)$$

and that in Eq. (85) the summation over $\lambda$ is assumed.

[7] We indicate explicitly all external helicity states, lepton helicity $\lambda$ is summed up.

$$M_{+-}^{+-} = 2mx_1 \left( A_2 \frac{R_2}{x_2 X_3} + \frac{Q}{a_1 a_{12}} \right) ,$$
$$M_{+-}^{-+} = 2m \frac{x_2}{X_3} \left( A_2 \frac{K_1}{x_1} - \frac{Q}{b_{12} b_2} \right) ,$$
$$M_{+-}^{--} = 0 , \qquad (95)$$
$$M_{+-}^{++} = -\frac{1}{1-x_1} \left( X_3 \, M_{+-}^{+-} + M_{+-}^{-+} \right)^* . \qquad (96)$$

All expressions are either identical [Eqs.(92), (93), (95)] to the amplitudes in Ref. [24] or can be transformed [Eqs.(94), (96)] after some algebra to those amplitudes.

As a result, we obtain all eight independent helicity amplitudes in the form[8]

$$\mathcal{M}_{+\pm}^{++} = (1 + \mathcal{P}_{12}) \, M_{+\pm}^{++} , \;\; \mathcal{M}_{++}^{--} = X_3 \left( \mathcal{M}_{++}^{++} \right)^* ,$$
$$\mathcal{M}_{+\pm}^{+-} = M_{+\pm}^{+-} + \mathcal{P}_{12} M_{+\pm}^{-+} , \;\; \mathcal{M}_{+\pm}^{-+} = \mathcal{P}_{12} \mathcal{M}_{+\pm}^{+-} , \qquad (97)$$
$$\mathcal{M}_{+-}^{--} = 0 .$$

The amplitudes are explicitly proportional to $Q$ or to the functions $A_2$ and $\tilde{A}_2$. Therefore, they vanish $\propto |\mathbf{q}_\perp|$ in the limit $|\mathbf{q}_\perp| \to 0$.

The spin–flip amplitudes (with $\lambda_1 = -\lambda_3$) are proportional to the electron mass $m$ and, therefore, they are negligible compared to the spin non–flip ones for not too small scattering angles

$$\frac{m}{x_{1,2} E_1} \ll \theta_{1,2} \ll 1 , \;\; \frac{m}{X_3 E_1} \ll \theta_3 \ll 1 . \qquad (98)$$

We also note the explicit Bose symmetry between the two photons in the amplitudes (98):

$$\mathcal{M}_{\lambda_1 \lambda_3}^{\Lambda_1 \Lambda_2}(K_1, x_1; K_2, x_2) = \mathcal{M}_{\lambda_1 \lambda_3}^{\Lambda_2 \Lambda_1}(K_2, x_2; K_1, x_1) . \qquad (99)$$

## 6 Impact factor for the multiple bremsstrahlung

$e(p_1) + \gamma^*(q) \to e(p_3) + \gamma(k_1) + \ldots + \gamma(k_n)$

The generalization of the results obtained in Sects. 4 and 5 to the bremsstrahlung of $n$ photons can be done straightforwardly. To demonstrate this, we consider the case $n = 3$ (Fig. 14) which clearly shows all nontrivial points of the multiple bremsstrahlung.

The helicity states of the initial and final electrons $\lambda_{1,3}$ and of the final photons $\Lambda_{1,2,3}$ are indicated explicitly in the impact factor:

$$J_1 = \sqrt{2} \, (4\pi\alpha)^2 \qquad (100)$$
$$\times \, X_3 \, \mathcal{M}_{\lambda_1 \, \lambda_3}^{\Lambda_1 \, \Lambda_2 \, \Lambda_3} (x_1, x_2, x_3, k_{1\perp}, k_{2\perp}, k_{3\perp}, p_{3\perp}) \, \Phi .$$

[8] To clarify the notation we stress that in Eqs. (98) with given polarizations the operator $\mathcal{P}_{12}$ simply interchanges the indices $1 \leftrightarrow 2$ and

$$\mathcal{P}_{12} A_2 = \frac{X_3}{a_2 a_{12}} - \frac{1 - x_2}{a_2 b_1} + \frac{1}{b_1 b_{12}} .$$

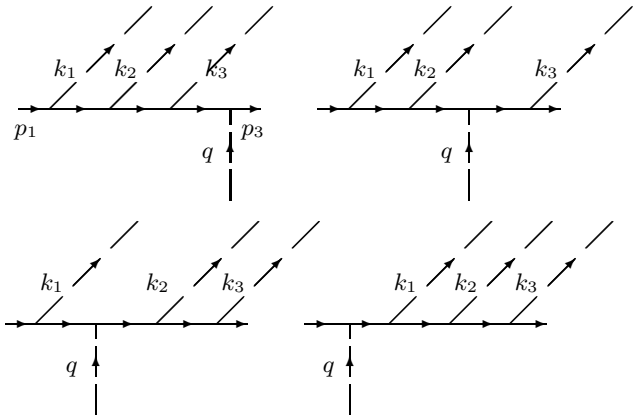


**Fig. 14.** Feynman diagrams for the impact factor related to the triple bremsstrahlung, diagrams with the exchange of the final photons have to be added.

where $\Phi$ has the form (80). The quantities $J_1$ and $\mathcal{M}$ do not depend on $s$, but depend only on the energy fractions

$$x_{1,2,3} = \omega_{1,2,3}/E_1 , \;\; X_3 = E_3/E_1 , \;\; x_1 + x_2 + x_3 + X_3 = 1$$

and on the transverse momenta of the final particles in the first jet with

$$q_\perp = \sum_{i=1}^{3} k_{i\perp} + p_{3\perp} .$$

For the denominators of the propagators in the diagrams of Fig. 14 we use the notations $(i, j = 1, 2, 3)$

$$\begin{aligned} a_i &= -(p_1 - k_i)^2 + m^2 , \\ b_i &= (p_3 + k_i)^2 - m^2 , \\ a_{ij} &= -(p_1 - k_i - k_j)^2 + m^2 , \\ b_{ij} &= (p_3 + k_i + k_j)^2 - m^2 , \\ a_{123} &= -(p_1 - k_1 - k_2 - k_3)^2 + m^2 , \\ b_{123} &= (p_3 + k_1 + k_2 + k_3)^2 - m^2 . \end{aligned} \qquad (101)$$

Just as in Sect. 5.2, we obtain

$$\mathcal{M} = (1 + \mathcal{P})(M + \tilde{M}) , \qquad (102)$$
$$\mathcal{P} = \mathcal{P}_{12} + \mathcal{P}_{23} + \mathcal{P}_{13} + \mathcal{P}_{13}\mathcal{P}_{12} + \mathcal{P}_{13}\mathcal{P}_{23} ,$$

$$\begin{aligned} X_3 M = {} & \frac{X_3}{a_1 a_{12} a_{123}} \, V(p_1, k_1) \\ & \times V(p_1 - k_1, k_2) \, V(p_1 - k_1 - k_2, k_3) - \\ & - \frac{1 - x_1 - x_2}{a_1 a_{12} b_3} \, V(p_1, k_1) \\ & \times V(p_1 - k_1, k_2) V(p_1 - k_1 - k_2 + q, k_3) + \\ & + \frac{1 - x_1}{a_1 b_{23} b_3} \, V(p_1, k_1) \\ & \times V(p_1 - k_1 + q, k_2) V(p_1 - k_1 - k_2 + q, k_3) - \\ & - \frac{1}{b_{123} b_{23} b_3} \, V(p_1 + q, k_1) \\ & \times V(p_1 - k_1 + q, k_2) V(p_1 - k_1 - k_2 + q, k_3) , \end{aligned} \qquad (103)$$

$$
\begin{aligned}
X_3\tilde{M} = &-\frac{X_3}{a_{12}a_{123}}\,\frac{\tilde{V}(p_1,k_1)\,\tilde{V}(p_1-k_1,k_2)}{4(E_1-\omega_1)^2}\\
&\times V(p_1-k_1-k_2,k_3)-\\
&-\frac{X_3}{a_{12}a_{123}}\,V(p_1,k_1)\\
&\times\frac{\tilde{V}(p_1-k_1,k_2)\tilde{V}(p_1-k_1-k_2,k_3)}{4(E_1-\omega_1-\omega_2)^2}+\\
&+\frac{1-x_1-x_2}{a_{12}b_3}\,\frac{\tilde{V}(p_1,k_1)\,\tilde{V}(p_1-k_1,k_2)}{4(E_1-\omega_1)^2}\\
&\times V(p_1-k_1-k_2+q,k_3)+\\
&+\frac{1-x_1}{a_1b_{23}}\,V(p_1,k_1)\\
&\times\frac{\tilde{V}(p_1-k_1+q,k_2)\tilde{V}(p_1-k_1-k_2+q,k_3)}{4(E_1-\omega_1-\omega_2)^2}-\\
&-\frac{1}{b_{123}b_3}\,\frac{\tilde{V}(p_1+q,k_1)\,\tilde{V}(p_1-k_1+q,k_2)}{4(E_1-\omega_1)^2}\\
&\times V(p_1-k_1-k_2+q,k_3)-\\
&-\frac{1}{b_{123}b_{23}}\,V(p_1+q,k_1)\\
&\times\frac{\tilde{V}(p_1-k_1+q,k_2)\tilde{V}(p_1-k_1-k_2+q,k_3)}{4(E_1-\omega_1-\omega_2)^2}\,.
\end{aligned}
\tag{104}
$$

To show that $J_1$ vanishes as $\propto q_\perp$ in the limit $q_\perp\to 0$, we follow the same line of action as in the previous section. This gives

$$
\begin{aligned}
X_3M &= A_3\,V(p_1,k_1)\,V(p_1-k_1,k_2)V(p_1-k_1-k_2,k_3)+\\
&\quad+q_\perp B_3\,,\\
X_3\tilde{M} &= \tilde{A}_3\,\frac{\tilde{V}(p_1,k_1)\,\tilde{V}(p_1-k_1,k_2)}{4(E_1-\omega_1)^2}V(p_1-k_1-k_2,k_3)+\\
&\quad+\tilde{A}'_3\,V(p_1,k_1)\,\frac{\tilde{V}(p_1-k_1,k_2)\tilde{V}(p_1-k_1-k_2,k_3)}{4(E_1-\omega_1-\omega_2)^2}+\\
&\quad+q_\perp\tilde{B}_3
\end{aligned}
\tag{105}
$$

where

$$
\begin{aligned}
A_3 &= \frac{X_3}{a_1a_{12}a_{123}}-\frac{1-x_1-x_2}{a_1a_{12}b_3}+\frac{1-x_1}{a_1b_{23}b_3}-\frac{1}{b_{123}b_{23}b_3}\,,\\
\tilde{A}_3 &= -\frac{X_3}{a_{12}a_{123}}+\frac{1-x_1-x_2}{a_{12}b_3}-\frac{1}{b_{123}b_{23}}\,,\\
\tilde{A}'_3 &= -\frac{X_3}{a_{12}a_{123}}+\frac{1-x_1}{a_1b_{23}}-\frac{1}{b_{123}b_{23}}
\end{aligned}
\tag{106}
$$

and the 4–vectors $B_3$ and $\tilde{B}_3$ can be easily found from Eqs. (104)–(106). The quantities $A_3$, $\tilde{A}_3$ and $\tilde{A}'_3$ vanish in the limit of small $q_\perp$

$$
A_3\propto q_\perp\,,\quad \tilde{A}_3\propto q_\perp\,,\quad \tilde{A}'_3\propto q_\perp\,,
\tag{107}
$$

the transverse 4–vectors $B_3$ and $\tilde{B}_3$ remain finite in this limit.

Again, Eq. (103) with relations (105) is a very simple and compact expression for all 32 helicity states where all individual large (compared to $q_\perp$) contributions have been cancelled.

## 7 Some general properties of bremsstrahlung impact factors

We discuss now some general properties of impact factors for the emission of real photons using mainly the double bremsstrahlung as example. For that case Eqs. (79), (84) and (87) define a simple, compact and transparent expression for the vertex factor which allows to obtain immediately all general properties obtained in Ref. [24] only after lengthy calculations. All those properties are directly related to the corresponding properties of vertices discussed in Sect. 3.3.

1) Bremsstrahlung amplitudes or impact factors with a maximal change of helicities are absent since in this case at least one transition vertex has to appear with a maximal change of its helicities (= 2) as well. Thus we have

$$
\mathcal{M}=0\ \text{ for }\ \max|\Delta\lambda|=n+1
\tag{108}
$$

where $\Delta\lambda=\sum_{i=1}^n\Lambda_i+\lambda_3-\lambda_1$ is the change of helicity in the transition from the first initial lepton to the first jet. In the case of the double bremsstrahlung, this corresponds to

$$
\mathcal{M}^{--}_{+-}=\mathcal{M}^{++}_{-+}=0\,.
$$

2) If one of the final particles in the jet (including the final lepton) becomes hard ($\omega_i\to E_1$ or $E_3\to E_1$) the sign of the helicity of the initial lepton coincides with that of the helicity of the hard final particle. This is the consequence of properties 2) and 3) discussed in Sect. 3.3.

3) In HNC amplitudes the sign of the helicity of at least one final photon has to coincide with the sign of the initial lepton helicity

$$
\mathcal{M}^{\Lambda_1\cdots\Lambda_n}_{\lambda_1\ -\lambda_1}\propto\delta_{\Lambda_i,2\lambda_1}\,.
\tag{109}
$$

4) The dependence of the whole amplitude $M$ on complex parameters of the form $z$ and $z^*$ defined in (52) can be easily reproduced for the whole amplitude using Eq. (60).

5) As can be seen from Eqs. (51), (54) and (55), the $\tilde{V}$ vertex may contribute only if the electron line connects two vertices with the emission of real photons. Both these adjacent vertices are of HNC type transitions so that the original lepton helicity is reestablished after passing these two vertices going along the lepton line. In our example, this happens for the two independent amplitudes (contributions including the $A'_2$ factor):

$$
\mathcal{M}^{+-}_{++}=\left(\mathcal{M}^{-+}_{--}\right)^*\,,\quad \mathcal{M}^{-+}_{++}=\left(\mathcal{M}^{+-}_{--}\right)^*\,.
$$

Since the number of real photons is 2 in that case, initial and final lepton helicities have to coincide for those amplitudes.

6) It is known that for soft photons (approximation of classical currents) the bremsstrahlung matrix element factorizes into a term responsible for the soft photon times an amplitude without the soft photon. In our approach this can can be easily realized using the following arguments. The form of a vertex in the soft photon limit is given by

Eq. (58). Furthermore, a virtual electron propagator close to a soft photon might have an infrared singularity only, if the soft photon is either at the beginning or the end of the electron line in a Feynman diagram. This has also the consequence that only those diagrams can contribute to the soft photon limit. Therefore, for a soft photon at the beginning of the electron line we have the vertex

$$V(p_1,k_1)\to -\frac{2}{x_1}\,(e_\perp^{(\Lambda_1)\,*}k_{1\perp})\;\delta_{\lambda_1\lambda}=2(e^{(\Lambda_1)\,*}p_1)\;\delta_{\lambda_1\lambda}$$

and the denominator of the corresponding electron propagator

$$(p_1-k_1)^2-m^2=-2p_1k_1$$

(and analogously for the soft photon at the end of the electron line). The remaining part of the amplitude is then taken at $k_1=0$ and represents the impact factor for $n-1$ bremsstrahlung photons. As a result, we get the factorization property for the impact factors (assuming the first photon being soft):

$$\begin{aligned}&J_1\left(e_{\lambda_1}(p_1)+\gamma^*(q)\to e_{\lambda_3}(p_3)+\sum_{i=1}^{n}\gamma_{\Lambda_i}(k_i)\right)\to\\&\to\sqrt{4\pi\alpha}\left(\frac{e^{(\Lambda_1)\,*}p_1}{p_1k_1}-\frac{e^{(\Lambda_1)\,*}p_3}{p_3k_1}\right)\\&\times\;J_1\left(e_{\lambda_1}(p_1)+\gamma^*(q)\to e_{\lambda_3}(p_3)+\sum_{i=2}^{n}\gamma_{\Lambda_i}(k_i)\right).\end{aligned}\tag{110}$$

The generalization to $m$ soft (first) photons out of $n$ bremsstrahlung photons is obvious:

$$\begin{aligned}&J_1\left(e_{\lambda_1}(p_1)+\gamma^*(q)\to e_{\lambda_3}(p_3)+\sum_{i=1}^{n}\gamma_{\Lambda_i}(k_i)\right)\to\\&\to(4\pi\alpha)^{\frac{m}{2}}\left\{\prod_{i=1}^{m}\left(\frac{e^{(\Lambda_i)\,*}p_1}{p_1k_i}-\frac{e^{(\Lambda_i)\,*}p_3}{p_3k_i}\right)\right\}\\&\times\;J_1\left(e_{\lambda_1}(p_1)+\gamma^*(q)\to e_{\lambda_3}(p_3)+\sum_{i=m}^{n}\gamma_{\Lambda_i}(k_i)\right).\end{aligned}\tag{111}$$

7) For a process with the emission of $n$ real photons we have the relation between the impact factors for initial positron and electron:

$$\begin{aligned}&J_1(e^+_{\lambda_1}+\gamma^*\to e^+_{\lambda_3}+\gamma_{\Lambda_1}+...+\gamma_{\Lambda_n})=\\&=(-1)^{n+1}\,J_1(e^-_{\lambda_1}+\gamma^*\to e^-_{\lambda_3}+\gamma_{\Lambda_1}+...+\gamma_{\Lambda_n}).\end{aligned}\tag{112}$$

This may be easily proven repeating the arguments given for the single bremsstrahlung in Sect. 4.

8) Let us consider the connection between the impact factor $J_1$ for the first jet discussed in Sect. 3—6 and the impact factor $J_2$ for the second jet. If the impact factor $J_1$ is related to the process

$$e_{\lambda_1}(p_1)+\gamma^*(q)\to e_{\lambda_3}(p_3)+\gamma_{\Lambda_1}(k_1)+\ldots+\gamma_{\Lambda_n}(k_n)\,,$$

it is a function of the following parameters

$$J_1\equiv J_1(\lambda_1;\,\lambda_3,X_3,p_{3\perp};\,\Lambda_1,x_1,k_{1\perp};\,\ldots;\,\Lambda_n,x_n,k_{n\perp})$$

where $X_3=E_3/E_1$ and $x_j=\omega_j/E_1$. The impact factor $J_2$, related to the process

$$e_{\lambda_2}(p_2)+\gamma^*(-q)\to e_{\lambda_4}(p_4)+\gamma_{\tilde\Lambda_1}(\tilde k_1)+\ldots+\gamma_{\tilde\Lambda_n}(\tilde k_n)\,,$$

depends on the parameters

$$J_2\equiv J_2(\lambda_2;\,\lambda_4,Y_4,p_{4\perp};\,\tilde\Lambda_1,\tilde y_1,\tilde k_{1\perp};\,\ldots;\,\tilde\Lambda_n,\tilde y_n,\tilde k_{n\perp})$$

where $Y_4=E_4/E_2$ and $\tilde y_j=\tilde\omega_j/E_2$. Any 4–vector $\tilde k=(\omega,\,\mathbf{k}_\perp,\,-k_z)$ for a particle in the second jet can be obtained from the 4–vector $k=(\omega,\,\mathbf{k}_\perp,\,k_z)$ for a particle in the first jet by spatial inversion and further rotation by an angle $\pi$ around the new $z$-axis. Since this operation changes the signs of helicities of leptons and photons, the impact factor $J_2$ is derived from $J_1$ by the following substitution rule:

$$\begin{aligned}J_2=J_1(&-\lambda_2;\,-\lambda_4,Y_4,p_{4\perp};\,-\tilde\Lambda_1,\tilde y_1,\tilde k_{1\perp};\,\ldots\\&\ldots;\,-\tilde\Lambda_n,\tilde y_n,\tilde k_{n\perp}).\end{aligned}\tag{113}$$

## 8 Summary

In the present paper we have formulated a new effective method to calculate all helicity amplitudes for bremsstrahlung jet–like QED processes at tree level.

The jet kinematic conditions here considered (2) provide the main contribution to the total cross sections of these processes at high energy. Within this kinematics, it is possible to obtain simple expressions of helicity amplitudes with an accuracy defined by (3). In this region, these amplitudes can be presented in the simple factorized form (4), where the impact factors $J_1$ or $J_2$ are proportional to the scattering amplitudes of the first or second initial lepton with the virtual exchanged photon.

The main advantage of our method consists in using simple universal "building blocks" — transition vertices with *real* leptons — which are matrices with respect to lepton helicities. Those vertices replace efficiently the spinor structure involving leptons of small virtuality in the impact factors, making the calculations short and transparent for any final helicity state. In the calculations we exploit a convenient decomposition of all 4–momenta of the reaction into large and small components involving Sudakov (or light-cone) variables.

The vertices themselves or their allowed combinations with well–defined prefactors (see discussion in Sect. 3.1) are finite in the high energy limit $s\to\infty$. In the case of bremsstrahlung we have found that only three nonzero transition vertices are required. The calculation of the vertices can be conveniently performed using the spinor or chiral representation of bispinors and $\gamma$–matrices. The properties of the vertices, discussed in Sect. 3.3, determine all nontrivial general properties of the helicity amplitudes described in Sect. 7.

By construction, the impact factors are finite in the high energy limit and depend only on energy fractions and transverse momenta of particles in the final jet, and on helicities of all real photons and leptons.

In Sections 4–6 we have calculated the impact factors for single, double and triple bremsstrahlung, following the same principles. In a first step, we use the allowed vertices to write down the corresponding impact factors, see Eqs. (63), (84), (85) and (103)–(105). In the next step, we use gauge invariance with respect to the virtual photon of 4–momentum $q$ and rearrange impact factors into a form in which all individual large (compared to $q_\perp$) contributions have been cancelled, see Eqs. (68), (75), (87), (98) and (105). Let us stress here again that the known results for bremsstrahlung helicity amplitudes to order $e^2$ and $e^3$ are now obtained almost immediately using this new method, while handling the spinor structure directly leads to cumbersome and tedious calculations in the case, for instance, of double photon bremsstrahlung. The result of order $e^4$ for the triple bremsstrahlung in one direction is completely new.

We have also defined rules to go over from impact factors with initial electrons to those with positrons [see Eq. (113)] and from the impact factors for the first jet to that for second jet [Eq. (113)].

Those rules together with the found impact factors allows us to give a complete analytic and compact description of all helicity amplitudes in $e^-e^\pm$ scattering with the emission of up to three photons in one lepton direction, where in the last case $2^5 \times 2^5$ different helicity amplitudes are involved.

Since by construction individual large contributions (compared to $q_\perp$) have been rearranged into finite expressions, the expressions obtained for the amplitudes are very convenient for numerical calculations of various cross sections.

Until now we have formulated our new method only for the case of photon bremsstrahlung from leptons. A next paper will be devoted to QED processes with production of lepton pairs [46].

## Acknowledgements

We are grateful to S. Brodsky, V. Fadin, I. Ginzburg, L. McLerran and A. Vainshtein for useful discussions. This work is supported in part by INTAS (code 00-00679), RFBR (code 00-02-17592) and by S.–Petersburg grant (code E00-3.3-146).

## Appendix

In the Appendix we collect some useful formulae about *spinor or chiral* representation (see, for example, Ref. [44] and text-book [45] §20, 21, 26).

We start with the *standard* representation in which an electron with momentum $\mathbf{p}$, energy $E = \sqrt{\mathbf{p}^2 + m^2}$ and helicity $\lambda = \pm 1/2$ is described by the bispinor

$$u_{\mathbf{p}}^{(\lambda)} = \begin{pmatrix} \sqrt{E+m}\, w^{(\lambda)}(\mathbf{n}) \\ 2\lambda \sqrt{E-m}\, w^{(\lambda)}(\mathbf{n}) \end{pmatrix},$$
$$\mathbf{n} = \frac{\mathbf{p}}{|\,\mathbf{p}\,|} = (\sin\theta\cos\varphi,\, \sin\theta\sin\varphi,\, \cos\theta)\,.$$

The two-component spinors $w^{(\lambda)}(\mathbf{n})$ obey the equations

$$(\boldsymbol{\sigma}\mathbf{n})\, w^{(\lambda)}(\mathbf{n}) = 2\lambda\, w^{(\lambda)}(\mathbf{n})\,, \quad w^{(\lambda)+}(\mathbf{n})\, w^{(\lambda')}(\mathbf{n}) = \delta_{\lambda\lambda'}$$

and have the form

$$w^{(1/2)}(\mathbf{n}) = \begin{pmatrix} \mathrm{e}^{-\mathrm{i}\varphi/2}\cos\frac{\theta}{2} \\ \mathrm{e}^{\mathrm{i}\varphi/2}\sin\frac{\theta}{2} \end{pmatrix},$$
$$w^{(-1/2)}(\mathbf{n}) = \begin{pmatrix} -\mathrm{e}^{-\mathrm{i}\varphi/2}\sin\frac{\theta}{2} \\ \mathrm{e}^{\mathrm{i}\varphi/2}\cos\frac{\theta}{2} \end{pmatrix}$$

with properties

$$\sigma_y w^{(\lambda)\,*}(\mathbf{n}) = 2\lambda \mathrm{i} w^{(-\lambda)}(\mathbf{n})\,, \quad w^{(\lambda)}(-\mathbf{n}) = \mathrm{i} w^{(-\lambda)}(\mathbf{n})$$

(here $\boldsymbol{\sigma}$ are the Pauli matrices). The normalization conditions are

$$\bar{u}_{\mathbf{p}}^{(\lambda)} u_{\mathbf{p}}^{(\lambda')} = 2m\,\delta_{\lambda\lambda'}\,, \qquad \sum_\lambda u_{\mathbf{p}}^{(\lambda)} \bar{u}_{\mathbf{p}}^{(\lambda)} = \hat{p} + m\,.$$

For the initial electron with momentum $\mathbf{p}_1$ ($\mathbf{p}_2$) along (opposite) the $z$-axis we use $\theta = 0$ ($\theta = \pi$). For the final electron with momentum $\mathbf{p}_3$ in the first jet we use $\theta = \theta_3$ and for the final electron with $\mathbf{p}_4$ in the second jet $\theta = \pi - \theta_4$.

The Dirac matrices in the standard representation are defined as

$$\gamma^0 = \begin{pmatrix} 1 & 0 \\ 0 & -1 \end{pmatrix}, \quad \boldsymbol{\gamma} = \begin{pmatrix} 0 & \boldsymbol{\sigma} \\ -\boldsymbol{\sigma} & 0 \end{pmatrix}, \quad \gamma^5 = \begin{pmatrix} 0 & -1 \\ -1 & 0 \end{pmatrix}.$$

A positron with momentum $\mathbf{p}$, energy $E = \sqrt{\mathbf{p}^2 + m^2}$ and helicity $\lambda$ is described by the bispinor

$$v_{\mathbf{p}}^{(\lambda)} = C \left(\bar{u}_{\mathbf{p}}^{(\lambda)}\right)^T,$$

with the charge conjugation matrix

$$C = \gamma^2\gamma^0\,, \quad C = -C^T = C^{-1}\,, \quad C^{-1}\gamma_\mu C = -\gamma_\mu^T\,.$$

Therefore, for a positron we get the bispinor

$$v_{\mathbf{p}}^{(\lambda)} = \mathrm{i}\begin{pmatrix} \sqrt{E-m}\, w^{(-\lambda)}(\mathbf{n}) \\ -2\lambda\sqrt{E+m}\, w^{(-\lambda)}(\mathbf{n}) \end{pmatrix},$$

with the normalization conditions

$$\bar{v}_{\mathbf{p}}^{(\lambda)} v_{\mathbf{p}}^{(\lambda')} = -2m\,\delta_{\lambda\lambda'}\,, \quad \sum_\lambda v_{\mathbf{p}}^{(\lambda)} \bar{v}_{\mathbf{p}}^{(\lambda)} = \hat{p} - m\,.$$

At high energies the bispinors $u$ and $v$ in the standard representation have top and bottom components of the same order, $\sim \sqrt{E}$, with relative corrections $\sim m/E$.

A more simple and convenient structure of bispinors can be found in the spinor or chiral representation, the transition to which is given by the matrix

$$U = U^{-1} = \frac{1}{\sqrt{2}}\left(\gamma^0 - \gamma^5\right) = \frac{1}{\sqrt{2}}\begin{pmatrix} 1 & 1 \\ 1 & -1 \end{pmatrix}.$$

In the spinor representation the electron bispinor is

$$Uu_{\mathbf{p}}^{(\lambda)} = \frac{1}{\sqrt{2}} \begin{pmatrix} \left(\sqrt{E+m} + 2\lambda\sqrt{E-m}\,\right) w^{(\lambda)}(\mathbf{n}) \\ \left(\sqrt{E+m} - 2\lambda\sqrt{E-m}\,\right) w^{(\lambda)}(\mathbf{n}) \end{pmatrix}.$$

At high energies $E \gg m$ this bispinor has a large top component $\sim \sqrt{E}$ and a small bottom component $\sim (m/\sqrt{E})$ for $\lambda = +1/2$ and vice versa for $\lambda = -1/2$ what is very useful for analysis. Furthermore, in that representation the corrections to the high energy asymptotics

$$Uu_{\mathbf{p}}^{(\lambda)} \approx \sqrt{m} \begin{pmatrix} (2E/m)^{\lambda}\, w^{(\lambda)}(\mathbf{n}) \\ (2E/m)^{-\lambda}\, w^{(\lambda)}(\mathbf{n}) \end{pmatrix}$$

is of the relative order of $m^2/E^2$. The approximate formulae for the positron bispinor in that representation are

$$Uv_{\mathbf{p}}^{(\lambda)} \approx 2\mathrm{i}\lambda\sqrt{m} \begin{pmatrix} -(2E/m)^{-\lambda}\, w^{(-\lambda)}(\mathbf{n}) \\ (2E/m)^{\lambda}\, w^{(-\lambda)}(\mathbf{n}) \end{pmatrix},$$

$$Uv_{-\mathbf{p}}^{(\lambda)} \approx 2\lambda\sqrt{m} \begin{pmatrix} (2E/m)^{-\lambda}\, w^{(\lambda)}(\mathbf{n}) \\ -(2E/m)^{\lambda}\, w^{(\lambda)}(\mathbf{n}) \end{pmatrix}.$$

Omitting terms of the order of $\theta^2$, we obtain the following simple expression for the two–component spinor:

$$w^{(\lambda=+1/2)}(\mathbf{n}) = \begin{pmatrix} 1 \\ a \end{pmatrix} \mathrm{e}^{-\mathrm{i}\lambda\varphi},$$

$$w^{(\lambda=-1/2)}(\mathbf{n}) = \begin{pmatrix} a \\ 1 \end{pmatrix} \mathrm{e}^{-\mathrm{i}\lambda\varphi}$$

where

$$a = \lambda\,\theta\,\mathrm{e}^{2\mathrm{i}\lambda\varphi} = -\frac{1}{\sqrt{2}\,E}\; p_{\perp}\, e_{\perp}^{(-2\lambda)*}$$

and the 4–vector $e_{\perp}^{(\Lambda)}$ is given in (16).

To calculate the vertices (37), (38) and (43) in the spinor representation we need the two matrices

$$U\gamma^0 \hat{P}_2 U^{-1} = E_2 \begin{pmatrix} 1+\sigma_z & 0 \\ 0 & 1-\sigma_z \end{pmatrix},$$

$$U\gamma^0 \hat{e}_{\perp} U^{-1} = \begin{pmatrix} -\mathbf{e}_{\perp}\boldsymbol{\sigma}_{\perp} & 0 \\ 0 & \mathbf{e}_{\perp}\boldsymbol{\sigma}_{\perp} \end{pmatrix}.$$

## References


1. Zeroth-Order Design Report for the Next Linear Collider, Report No. SLAC-474 (1996); JLC Design Study, KEK Report 97-1 (1997); R.D. Heuer et al., Technical Design Report of 500 GeV Electron Positron Collider with Integrated X-Ray Facility (DESY 2001-011, March 2001); Physics Potential and Development of $\mu^+\mu^-$ Colliders, Ed. D. Cline (AIP Conference Proceedings 441 (1997))
2. G.L. Kotkin, A. Schiller, V.G. Serbo, Int. J. Mod. Phys. A **7** (1992) 4707
3. G. Racah, Nuovo Cim. **14** (1937) 93
4. P. Kessler, Nuovo Cim. **17** (1960) 809
5. G. Altarelli, F. Buccella, Nuovo Cim. **34** (1964) 1337; V.M. Baier, V.S. Fadin, V.A. Khoze, ZhETF **51** (1966) 1135
6. V.N. Baier, V.M. Galitsky, Phys. Lett. **13** (1964) 355; Pis'ma ZhTEF **2** (1965) 259; V.M. Baier, V.S. Fadin, V.A. Khoze, ZhETF **50** (1966) 1611;
7. L.N. Lipatov, G.V. Frolov, Pis'ma ZhETF **10** (1969) 399; Yad. Fiz. **13** (1971) 558
8. H. Cheng, T.T. Wu, Phys. Rev. D **1** (1970) 3414
9. V.G. Serbo, Pis'ma ZhETF **12** (1970) 50, 452
10. V.M. Budnev, I.F. Ginzburg, G.V. Meledin, V.G. Serbo, Yad. Fiz. **16** (1972) 362
11. E.A. Kuraev, L.N. Lipatov, Yad. Fiz. **16** (1972) 1060; Yad. Fiz. **20** (1974) 112
12. V.L. Chernyak, V.G. Serbo, Nucl. Phys. B **67** (1973) 464; B **77** (1974) 545
13. E.A. Kuraev, L.N. Lipatov, M.I. Strikman, Yad. Fiz. **18** (1973) 1270
14. V.M. Baier, V.S. Fadin, V.A. Khoze, Nucl. Phys. B **65** (1973) 381
15. G. Bonneau, F. Martin, Nucl. Phys. B **68** (1974) 367
16. G.L. Kotkin, V.G. Serbo, Yad. Fiz. **21** (1975) 785
17. J. Smith, J.A.M. Vermaseren, G. Grammer, Phys. Rev. D **15** (1977) 3280
18. E.A. Kuraev, V.S. Fadin, Preprint INP (Novosibirsk) 78-56 (1978)
19. C. Carimalo, P. Kessler, J. Parisi, Phys. Rev. D **20** (1979) 1957; 2170
20. E.A. Kuraev, A. Schiller, V.G. Serbo, Nucl. Phys. B **256** (1985) 189
21. E.A. Kuraev, A. Schiller, V.G. Serbo, Z. Phys. C **30** (1986) 237
22. I.F. Ginzburg, V.G. Serbo, Phys. Rev. D **49** (1994) 2623.
23. E.A. Kuraev, A. Schiller, V.G. Serbo, D.V. Serebryakova, Eur. Phys. J. C **4** (1998) 631
24. E.A. Kuraev, A. Schiller, V.G. Serbo, B.G. Shaikhatdenov, Nucl. Phys. B **570** (2000) 359
25. V.M. Budnev, I.F. Ginzburg, G.V. Meledin, V.G. Serbo, Phys. Rep. **15** C (1975) 181
26. V.N. Baier, V.S. Fadin, V.A. Khoze and E.A. Kuraev, Phys. Rep. **78** (1981) 293
27. P.A. Baikov et al., Proc. High Energy Physics and Quantum Field Theory, ed. B. Levchenko and V. Savrin, Moscow (1996); hep-ph/9701412
28. R. Kleiss, Nucl. Phys. B **241** (1984) 61; F.A. Berends et al., Nucl. Phys. B **264** (1986) 243; V.S. Fadin, E.A. Kuraev, A.N. Peryshkin, Preprint INP 86-91 (Novosibirsk, 1986); E.A. Kuraev, A.N. Peryshkin, Yad. Fiz. **42** (1986) 1195
29. G.R. Farrar, F. Neri, Phys. Lett **130** B (1983) 109
30. P.I. Golubnichy et al., Atomnaya Energiya **22** (1966) 168
31. I. Augustin et al., Preprint LAL-1249 (1971)
32. G. De Zorzi et al., Polarization at LEP, Preprint CERN 88-06, v. 2, p. 64 (1988)
33. G.L. Kotkin, S.I. Polityko, A. Schiller, V.G. Serbo, Phys. Lett. B **221** (1989) 96
34. C. Bini et al., Nucl. Instrum. Meth. A **349** (1994) 27
35. A. Courau, G. Pancheri, Phys. Lett. B **396** (1997) 287
36. C. Carimalo, P. Kessler, J. Parisi, Nucl. Phys. B **57** (1973) 582
37. I.F. Ginzburg, G.L. Kotkin, V.G. Serbo, V.I. Telnov, Nucl. Instrum. Meth. **205** (1983) 47

38. C. Carimalo, W. Da Silva, F. Kapusta, Nucl. Instrum. Meth. A **472** (2001) 185
39. I.F. Ginzburg, Nucl. Phys. B (Proc. Suppl.) A **51** (1996) 196
40. A.B. Arbuzov et al., Phys. Lett. B **394** (1997) 218
41. I.F. Ginzburg, A. Schiller, V.G. Serbo, Eur. Phys. J. C **18** (2001) 731
42. H. Burkhard, Proc. 3 Workshop on LEP Performance (Chamonix, January 10-16, 1993) CERN SL/93–19, ed. J. Poole, p. 117; Proc. 7 Advanced Beam Dynamics Workshop (Dubna, May 1995), p. 22; Y. Funakoshi, Proc. of Int. Workshop on B-Factories: Accelerators and Experiments, KEK Proc.93-7/June 1993, p. 66.
43. I.F. Ginzburg, S.L. Panfil, V.G. Serbo, Nucl. Phys. B **284** (1987) 685, ibid. B **296** (1988) 581; I.F. Ginzburg, D.Yu. Ivanov, Nucl. Phys. B **388** (1992) 376
44. R. Kleiss, W.J. Stirling, Nucl.Phys. B **262** (1985) 235
45. V.B. Berestetskii, E.M. Lifshitz, L.P. Pitaevskii, Quantum electrodynamics, Pergamon Press (Second English edition, 1994).
46. C. Carimalo, A. Schiller, V.G. Serbo, in preparation